growth on HF6 cells. Although the constitutively active mutants of STAT5A, the relatively stronger mutant STAT5A1*6 and weaker mutant STAT5A#2, enabled Ba/F3 cells (Ba/F3^{1*6}, Ba/F3$^{\#}$) to grow without IL-3 as reported earlier,[25,27,28] both failed to confer factor-independent growth on HF6 cells with limited elongation of survival time without IL-3 (Figures 3a and c). In contrast, the oncogenic *NRAS* mutant, *NRAS*^{G12V}, which had been detected in a case of *AML* with *MLL-SEPT6*,[20] enabled HF6 cells (HF6^{G12V}) to grow without IL-3, while it conferred no factor-independent growth on Ba/F3 with limited elongation of survival time without IL-3 (Figures 3b and c). In addition, Raf-1, a signal molecule downstream of Ras in Ras-MAPK cascades associated with malignant transformation, was tested with an activation-inducible system using Δ*Raf*-ER, consisting of the catalytic domain of human RAF-1 (ΔRaf) and the hormone-binding domain of the ER (Figure 3d), as described earlier.[28] Unlike transduced Ba/F3 (Ba/F3$^{\Delta Raf\text{-}ER}$) cells, transduced HF6 (HF6$^{\Delta Raf\text{-}ER}$) cells grew without IL-3 only in the presence of 4-hydroxy-tamoxifen (Figure 3e). In these HF6$^{\Delta Raf-ER}$ cells treated with 4-hydroxy-tamoxifen, STAT5A was not found to be secondarily activated by induction of activation of Raf/MAPK cascade in the absence of IL-3, whereas it was found to be weakly activated by stimulation with IL-3 for 15 min (data not shown).

Furthermore, we examined whether *Hoxa9*, which is one of the well-known target genes of *MLL* fusion proteins,[10,11,13,14] is involved in cooperation between *MLL* fusion protein and Ras/Raf/MAPK cascade. In the myeloid transformation assays, the murine BM progenitors immortalized by *Hoxa9* in the presence of IL-3 (named A9G) proliferated without IL-3 after retroviral transduction of *NRAS*^{G12V} (Figure 3b). In the inducible transformation system using Δ*Raf*-ER, transduced A9G

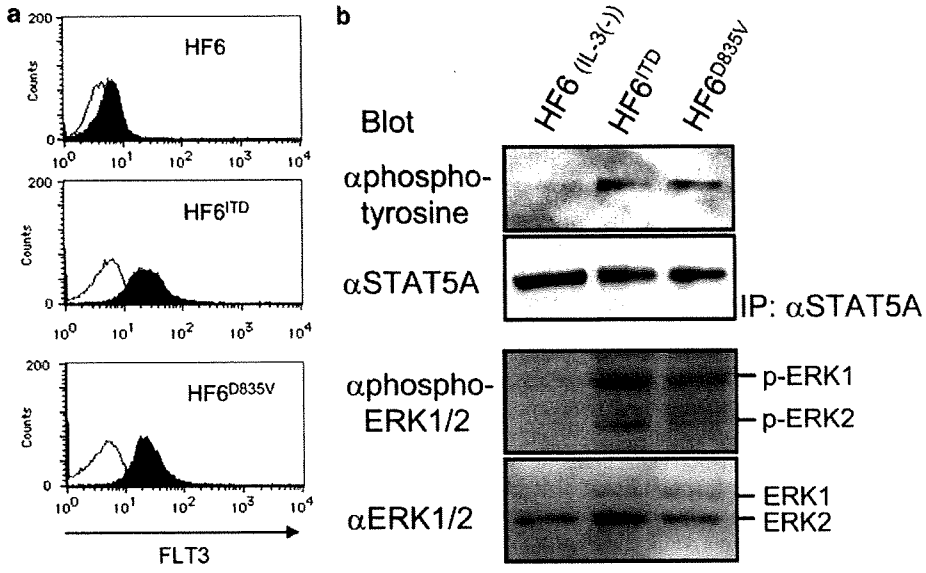

Figure 1 Characterization of signal transduction in the HF6 cells transformed by *FMS-like receptor tyrosine kinase 3* (*FLT3*) mutants. (**a**) Expression of each *FLT3* mutant in HF6 and their transformed cells. The shadow profiles and black lines represent fluorescence-activated cell sorting (FACS) staining obtained using the antibody specific to *FLT3* and its isotype control antibody, respectively. (**b**) Western blot analyses of proteins extracted from HF6 and their transformed cells after immunoprecipitation using the anti-signal transducer and activator of transcription 5A (STAT5A) antibody (upper two panels), and of the whole lysates (lower two panels). The parental HF6 cells had been deprived of interleukin-3 (IL-3) 8 h before harvest. The blot of the immunoprecipitated samples was probed with the anti-STAT5A antibody (upper bottom panel), followed by reprobe with 4G10 (the anti-phosphotyrosine antibody) (upper top panel). The blot of the whole lysates was probed with the anti-extracellular signal-related kinase (ERK)1/2 antibody (lower bottom panel), followed by reprobe with the anti-phospho-ERK1/2 antibody (lower top panel).

Figure 2 Differential effects of inhibition of cellular signal transduction on the HF6 cells transformed by *FMS-like receptor tyrosine kinase 3* (*FLT3*) mutants. (a) Effect of the retroviral transduction with the dominant negative mutant of signal transducer and activator of transcription 5A (dnSTAT5A) in pMXs-internal ribosomal entry site (IRES)-Kusabira-Orange (KO) on the transformed and parental HF6 cells. Viable cell numbers and KO expression were monitored daily after the transduction, and the averages of ratios of each KO-positive cell number at days 1, 2, 3 and 4 to that at day 1 are shown with s.d. (bars). (**b**) Intracellular flow cytometric analyses of phospho-STAT5 (Y694) on the transformed and parental HF6 cells transduced with dnSTAT5A in pMXs-IRES-KO. The density plots show expression of each intracellular antigen labeled with the Alexa Fluor 647-conjugated anti-phospho-STAT5 (Y694) (upper eight panels) or its isotype control (lower two panels) antibody versus expression of KO. As negative controls, nontransduced and mock-transduced HF6 cells were used, respectively (lower two panels using the isotype control antibody). As references, nontransduced HF6 cells were deprived of interleukin-3 (IL-3) for 8 h (HF6 (IL-3(−))), or stimulated with IL-3 for 15 min after the same deprivation (HF6 (IL-3(+))), and then used (lower two panels using the anti-phospho-STAT5 antibody). KO and Alexa Fluor 647 were detected using the FL2 and FL4 channels of the fluorescence-activated cell sorting (FACS) Calibur, respectively. (**c**) Effect of the various concentrations of mitogen-activated protein kinase (MAPK) kinase (MEK) inhibitor, U0126, on the transformed and the parental HF6 cells. The averages with s.d. (bars) of ratios of viable cell numbers in the presence of each concentration of U0126 to those in the absence of U0126 are shown. (**d**) Western blot analyses of the whole lysates extracted from the transformed HF6 cells treated with U0126. Both groups of transformed HF6 cells were treated with various concentrations (shown above each upper panel) of U0126 for 2 h and then harvested. Both blots were probed with the anti-phospho-extracellular signal-related kinase (ERK)1/2 antibody (each top panel), followed by reprobe with the anti-ERK1/2 antibody (each bottom panel).

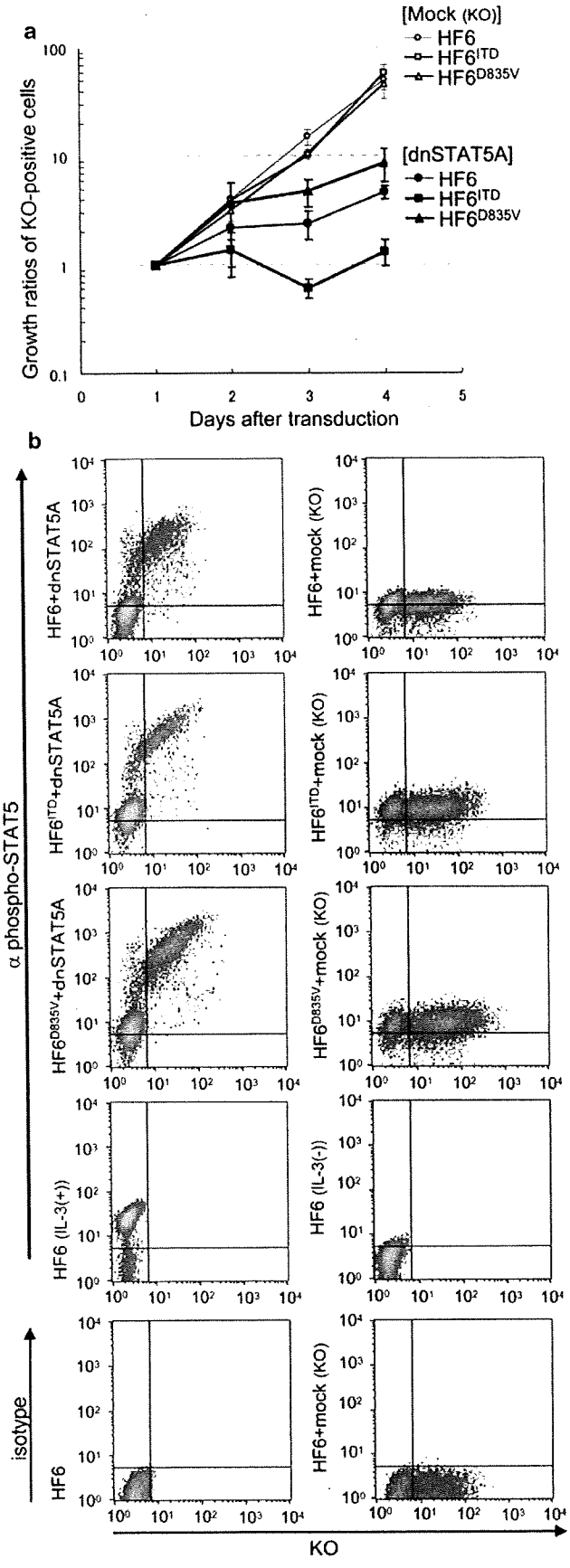
a
[Mock (KO)]
HF6
HF6ITD
HF6D835V
[dnSTAT5A]
HF6
HF6ITD
HF6D835V
Growth ratios of KO-positive cells
Days after transduction
b
α phospho-STAT5
HF6+dnSTAT5A
HF6+mock (KO)
HF6ITD+dnSTAT5A
HF6ITD+mock (KO)
HF6D835V+dnSTAT5A
HF6D835V+mock (KO)
HF6 (IL-3(+))
HF6 (IL-3(-))
isotype
HF6
HF6+mock (KO)
KO

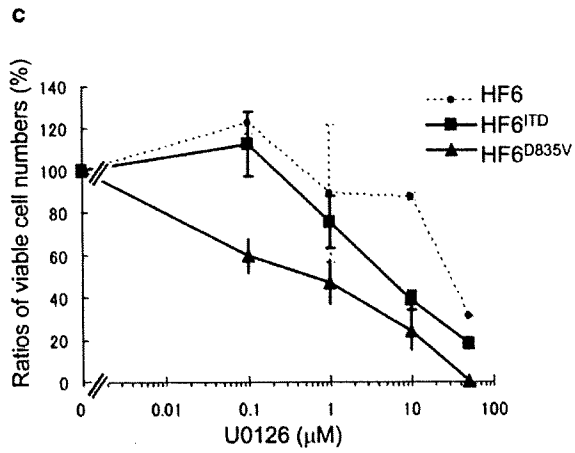
c
Ratios of viable cell numbers (%)
HF6
HF6ITD
HF6D835V
U0126 (μM)

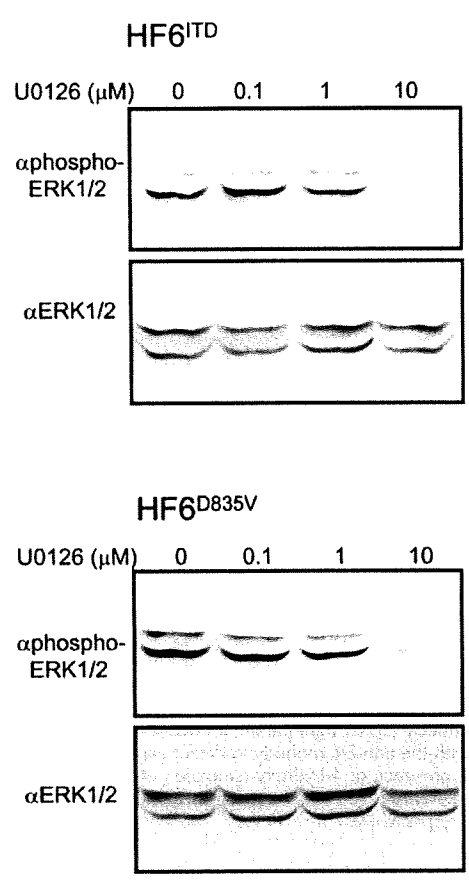
d
HF6ITD
U0126 (μM) 0 0.1 1 10
αphospho-ERK1/2
αERK1/2
HF6D835V
U0126 (μM) 0 0.1 1 10
αphospho-ERK1/2
αERK1/2

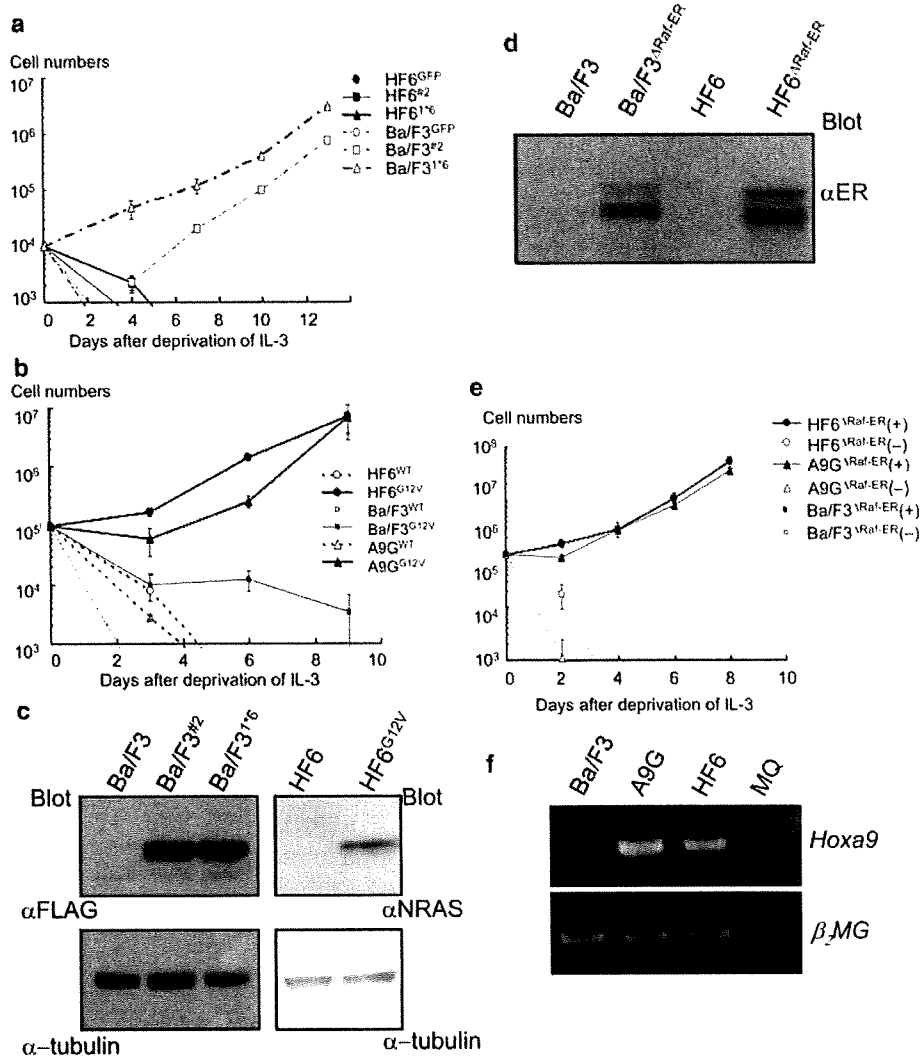

Figure 3 Transformation of the HF6 and A9G cells induced by direct activation of Ras/Raf/mitogen-activated protein kinase (MAPK) pathway. (**a**) Transformation assays of the HF6 and Ba/F3 cells expressing constitutively active forms of signal transducer and activator of transcription 5A (STAT5A) (#2 and 1*6). Green fluorescent protein (GFP) was used as a control. (**b**) Transformation assays of the HF6, A9G and Ba/F3 cells expressing wild-type (WT) *NRAS* or $NRAS^{G12V}$ (G12V). The averages of the number of viable cells with s.d. (bars) are shown in (**a**) and (**b**). (**c**, **d**) Western blot analyses of the whole lysates extracted from the transduced cells (see legends to panels (a) and (b)) in the absence of interleukin-3 (IL-3). (**c**) HF6 and Ba/F3 cells transduced with an inducible form of Raf (Δ*Raf*-estrogen receptor (ER)) (**d**) and their parental cells (**c**, **d**). The blot was probed with the anti-FLAG antibody to detect expression of ectopically expressed STAT5A mutants (upper left panel), or probed with the anti-*NRAS* antibody (upper right panel), followed by reprobe with the anti-α-tubulin antibody as internal control (lower panels) (**c**). The blot was also probed with the anti-ER antibody to detect expression of Δ*Raf*-ER (**d**). (**e**) Transformation assays of the HF6, A9G and Ba/F3 cells expressing Δ*Raf*-ER in the presence of 4-hydroxy-tamoxifen (4-OHT) (+) or vehicle control (−). The averages of the number of viable cells with s.d. (bars) are shown. (**f**) Analysis of *Hoxa9* transcripts in A9G cells using reverse transcriptase-PCR. Ba/F3 and HF6 cells were used as negative and positive controls, respectively.

Figure 4 Leukemogenesis induced by *mixed-lineage-leukemia* (*MLL*)-septin 6 (*SEPT6*) with $NRAS^{G12V}$ synergistically, but not with signal transducer and activator of transcription 5A (STAT5A)#2, *in vivo* under lethal conditioning. (**a**) Survival curves of mice transplanted with *MLL-SEPT6* and $NRAS^{G12V}$ (MS6/G12V; $n=6$), MS6 and *STAT5A*#2 (MS6/#2; $n=6$), MS6/GFP ($n=6$), neo/G12V ($n=6$), neo/#2 ($n=3$) and neo/GFP ($n=3$). (**b**) Representative macroscopic images of spleens obtained from each group of mice shown in (**a**). Scale bar 1 cm. (**c**, **d**) Representative histopathological analysis of morbid mice transplanted with MS6/#2, MS6/G12V (**c**, **d**), neo/G12V, and neo/#2 (**d**). Bone marrow (BM) cells (**c**) and paraffin sections of spleen (**d**) were stained with Wright-Giemsa and hematoxylin and eosin (H&E), respectively. Original magnification, × 200 (**c**) and × 40 (**d**); scale bars, 30 μm (c) and 200 μm (**d**). (**e**, **f**) Immunophenotype of BM or splenic (Sp) cells obtained from representative morbid mice transplanted with MS6/#2 (**e**, left panels), MS6/G12V (**e**, right panels), neo/G12V (**f**, left panels) and neo/#2 (**f**, right panels). The dot plots show each surface antigen labeled with a corresponding monoclonal antibody versus expression of GFP. Ly5.1, Gr-1, CD11b, Ter119, and c-Kit were labeled with phycoerythrin (PE)-conjugated and allophycocyanin (APC)-conjugated monoclonal antibodies, respectively. (**g**) Southern blot analysis to detect clonality (left panel) and proviral integration (right panel). Genomic DNA extracted from BM cells obtained from representative mice transplanted with MS6/G12V (lanes 4, 5, 9 and 10), MS6/GFP (lanes 2, 3, 7 and 8) and neo/GFP (5 months after transplantation; lanes 1 and 6) was digested with *Bam*HI (lanes 1–5) and *Nhe*I (lanes 6–10), respectively, and hybridized with the Neo probe. Oligoclonal bands of proviral integration and single bands of the proviral DNA are indicated by arrows and arrowheads, respectively.

(A9G$^{\Delta Raf-ER}$) cells grew without IL-3 only in the presence of 4-hydroxy-tamoxifen (Figure 3e). Expression level of *Hoxa9* in A9G cells was shown in comparison with those in Ba/F3 and HF6 (negative and positive controls, respectively) cells by reverse transcriptase-PCR (Figure 3f).

Taken together, these results *in vitro* suggested the essential role of activation of the Ras/Raf/MAPK cascade together with *Hoxa9* upregulated by *MLL* fusion proteins in the transformation of the cells expressing *MLL* fusion protein.

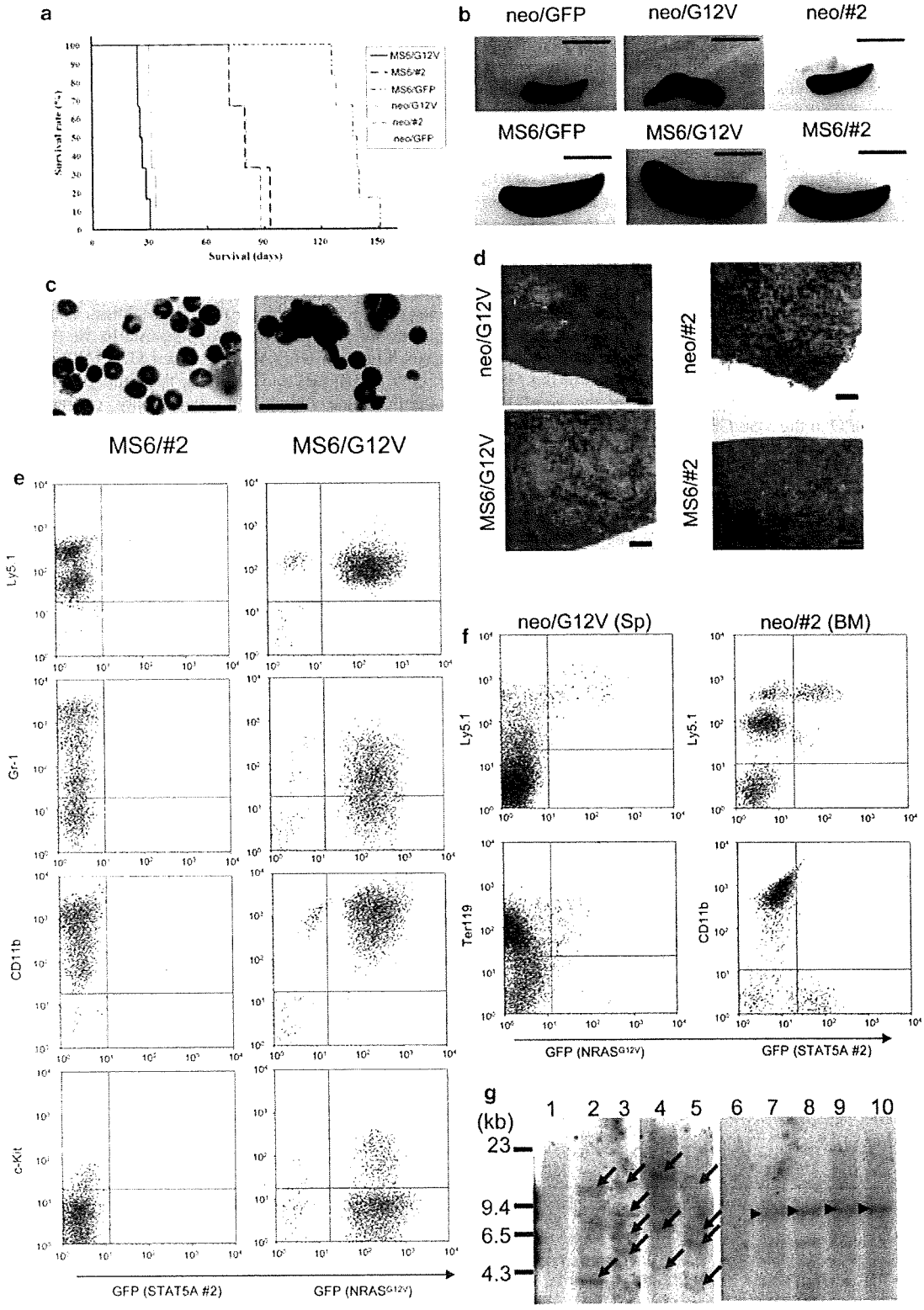

MLL *fusion proteins and oncogenic* NRAS *cooperate to induce acute leukemia, at least partly through aberrant expression of* Hoxa9

The findings on the transformation of HF6 cells *in vitro* led to the hypothesis that *MLL* fusion proteins might cooperate with activation of Ras to induce *AML in vivo*. To test this hypothesis, the oncogenic potential of $NRAS^{G12V}$ (G12V) or STAT5A#2 (#2) to cooperate with *MLL-SEPT6* (MS6) or *MLL-ENL* short form was examined in the leukemogenesis assays *in vivo* (Supplementary Figure 1). STAT5A1*6 was not used owing to its too strong oncogenic potential *in vivo* as reported earlier.[36] The transduction efficiencies of $NRAS^{G12V}$, STAT5A#2 and *MLL-ENL* were 30–50, 20–40 and 5–10%, respectively, as determined by GFP expression (data not shown).

The mice receiving the BM cells transduced with *MLL-SEPT6* and $NRAS^{G12V}$ (MS6/G12V) died with significantly shorter latencies (26 ± 2.4 days; $P<0.05$, log-rank test) than the MS6/GFP mice that died of MPD (137 ± 9.0 days) as described earlier,[6] but, unexpectedly, the neo/G12V mice died as early as the MS6/G12V mice (31 ± 1.4 days) (Figure 4a, Table 1, and data not shown). The MS6/#2 mice died with significantly shorter latencies (82 ± 11 days; $P<0.05$, log-rank test) than the MS6/GFP mice, but as early as the neo/#2 mice (80 ± 8.0 days) (Figure 4a and Table 1). Notably, the phenotypes of the MS6/G12V mice were very different from those of the neo/G12V mice and from MPD in the MS6/GFP mice, whereas those of the MS6/#2 mice were rather similar to MPD in the MS6/GFP mice than those of the neo/#2 mice.

The morbid MS6/G12V mice showed hepatosplenomegaly with various ranges of leukocytosis, anemia and thrombocytopenia, whereas the morbid neo/G12V mice showed no hepatomegaly but mild splenomegaly, and severe pancytopenia (Figure 4b and Table 1). Histopathological analyses of the morbid MS6/G12V mice showed that immature myelomonocytic blasts accounted for more than 30% of BM cells, and severely infiltrated the spleen and the liver (Figures 4c and d, and data not shown). Immunophenotyping analyses of the BM cells also revealed that a majority of these cells expressed GFP, which indicated expression of $NRAS^{G12V}$, with high level of CD11b, intermediate level of Gr-1 (a myeloid differentiation marker also known as Ly-6G) and low level of c-Kit (CD117, the receptor of stem cell factor) (Figure 4e). In addition, Southern blot analysis of genomic DNAs derived from the spleens of the MS6/G12V mice showed oligoclonal bands of proviral integration (Figure 4g). These results indicated that the MS6/G12V mice developed *AML* similar to the mice receiving BM cells transduced with *MLL-SEPT6* and *FLT3*-ITD, as described earlier.[6] In contrast, the morbid neo/G12V mice showed extremely hypocellular marrows and extramedullary hematopoiesis in the spleen, where a majority of the cells did not express Ly5.1 (Figure 4f), with little expression of *Hoxa9* in comparison with the morbid MS6/G12V mice (Supplementary Figure 3a). Thus, this finding suggested that, in our leukemogenesis assays under lethal conditioning, *NRAS* might develop BM aplasia presumably due to engraftment failure. Meanwhile, the MS6/#2 mice died of MPD, showing myeloid hyperplasia consisting predominantly of mature granulocytic elements in the BM cells, where a very small population (1.0%) expressed STAT5A#2, with splenomegaly similar to the MS6/GFP mice (Figures 4b–d, and Table 1). The neo/#2 mice showed neither hepatosplenomegaly nor hematological abnormalities in the peripheral blood, but relative myeloid hyperplasia in the BM, where only a small population (9.4%) expressed STAT5A#2 (Figures 4b and f, data not shown and Table 1), thus implying that STAT5A#2 might induce lethal BM abnormality owing to paracrine expression of some cytokines as in the earlier report using STAT5A1*6.[36]

To generalize leukemogenic cooperation between *MLL* fusion proteins and oncogenic *NRAS* and avoid the early death caused by transduction of $NRAS^{G12V}$, the BM cells transduced with *MLL-ENL* and/or oncogenic *NRAS* were also transplanted into recipient mice under sublethal conditioning. The *MLL-ENL* short form was used for leukemogenesis assays under sublethal conditioning with oncogenic *NRAS* ($NRAS^{G12V}$), in which retroviral vectors were exchanged, so that the expression of GFP indicated that of *MLL-ENL* (Supplementary Figure 1). These leukemogenesis assays under sublethal conditioning confirmed that the combination of *MLL-ENL* and $NRAS^{G12V}$ reproduced *AML*, and that *MLL-ENL* (and puro) induced the phenotype of MPD (Figures 5a, b and d, and Table 1). Meanwhile, $NRAS^{G12V}$

Table 1 Characteristics of the morbid mice transplanted with hematopoietic progenitors transduced with *MLL* fusion genes or *Hoxa9*, and/or either $NRAS^{G12V}$ or STAT5A #2

Mouse	*Latency (days)*	*Liver (g)*	*Spleen (g)*	*Thymus (g)*	*WBC (per μl)*	*Hb (g per 100 ml)*	*Plt (× 10^4 per μl)*
Lethal conditioning							
MS6/G12V ($n=6$)	26 ± 2.4	1.60 ± 0.35	0.31 ± 0.07	0.020 ± 0.012	74 600 ± 62 900	4.2 ± 1.0	4.0 ± 3.9
MS6/#2 ($n=3$)[a]	82 ± 11	0.98 ± 0.43	0.32 ± 0.03	0.019 ± 0.006	73 100	5.3	4.4
MS6/GFP ($n=6$)	137 ± 9.0	1.54 ± 0.69	0.26 ± 0.09	0.037 ± 0.005	309 000 ± 263 000	7.0 ± 6.6	8.0 ± 5.7
neo/G12V ($n=6$)	31 ± 1.4	1.04 ± 0.25	0.25 ± 0.08	0.030 ± 0.030	4600 ± 1800	2.5 ± 0.3	0.5 ± 0.4
neo/#2 ($n=3$)[a]	80 ± 8.0	0.66 ± 0.16	0.08 ± 0.06	0.011 ± 0.001	9800	18.8	58.2
neo/GFP ($n=3$)	NA	1.36 ± 0.11	0.09 ± 0.01	0.051 ± 0.010	12 000 ± 4700	14.7 ± 0.6	81 ± 13
A9/G12V ($n=4$)	28 ± 7.5	1.93 ± 0.56	0.44 ± 0.16	0.033 ± 0.030	76 300 ± 56 700	4.5 ± 2.7	1.0 ± 0.6
A9/GFP ($n=6$)	NA	NT	NT	NT	21 200 ± 5400	17.3 ± 2.4	66 ± 4.7
puro/GFP ($n=3$)	NA	1.48 ± 0.21	0.06 ± 0.01	0.049 ± 0.022	12 000 ± 3400	13.6 ± 1.5	81 ± 19
Sublethal conditioning							
MEs/G12V ($n=10$)	21 ± 3.9	2.56 ± 0.45	0.51 ± 0.10	0.043 ± 0.020	164 000 ± 131 000	7.2 ± 2.5	11 ± 4.5
MEs/puro ($n=5$)	89 ± 11	1.89 ± 0.58	0.44 ± 0.11	0.043 ± 0.006	99 000 ± 53 000	7.4 ± 2.9	9.1 ± 3.1
GFP/G12V ($n=5$)[b]	89 ± 10	0.90 ± 0.31	0.06 ± 0.03	0.63 ± 0.35	22 000 ± 1000	13.6 ± 1.7	97
GFP/puro ($n=3$)	NA	NT	NT	NT	NT	NT	NT

Abbreviations: GFP, green fluorescent protein; Hb, hemoglobin; MEs, *MLL-ENL* short form; NA, not applicable; NT, not tested; Plt, platelet; WBC, white blood cell.
Averages with s.d. are shown.
[a]Blood cell counts of only one morbid mouse were performed.
[b]One mouse developing acute leukemia and thymoma was excluded, owing to the remarkably increased number of WBCs and hepatosplenomegaly. The platelet count of only one morbid mouse was determined.

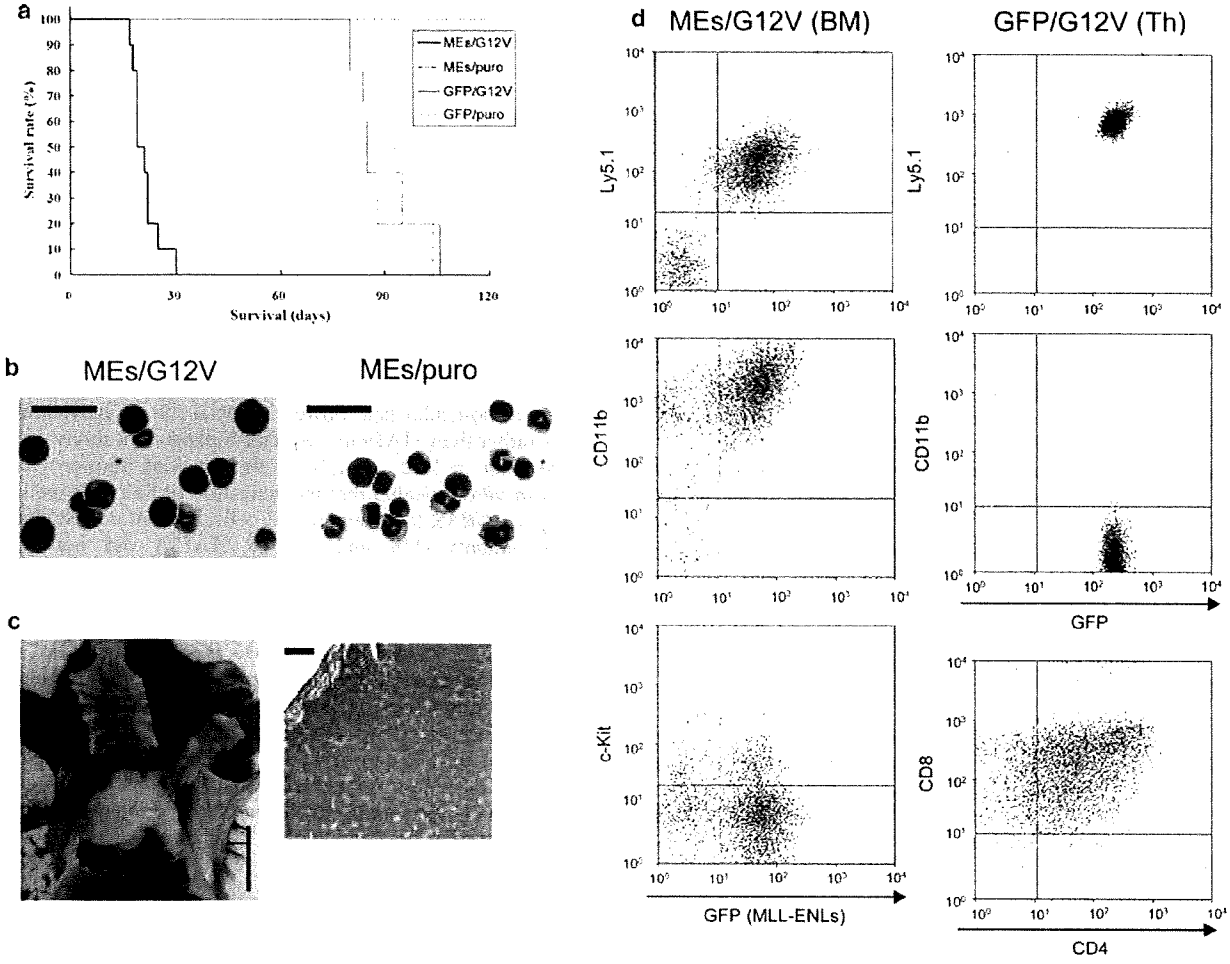

Figure 5 Leukemogenesis assays under sublethal conditioning using *mixed-lineage-leukemia/eleven nineteen leukemia* (*MLL-ENL*) and $NRAS^{G12V}$. (**a**) Survival curves of mice transplanted with a short form of *MLL-ENL* (MEs) and $NRAS^{G12V}$ (MEs/G12V) ($n=10$), MEs/puro ($n=5$), GFP/G12V ($n=5$) and green fluorescent protein (GFP)/puro ($n=3$). (**b**) Representative cytospin preparations of bone marrow (BM) cells obtained from morbid MEs/G12V and MEs/puro mice. The cells were stained with Wright-Giemsa. Original magnification 200×; Scale bars 30 μm. (**c**) Representative histopathologic images of thymus obtained from the GFP/G12V mouse. A paraffin section of the thymus was stained with hematoxylin and eosin (H&E). Original magnification, ×40; vertical and horizontal scale bars, 1 cm and 200 μm, respectively. (**d**) Immunophenotype of BM and thymic (Th) cells obtained from representative morbid MEs/G12V and GFP/G12V mice. The dot plots show each surface antigen labeled with a corresponding monoclonal antibody versus expression of GFP or CD4. Ly5.1, CD11b, CD4, and c-Kit and CD8 were labeled with phycoerythrin (PE)-conjugated and allophycocyanin (APC)-conjugated monoclonal antibodies, respectively.

(and GFP) led to thymoma, sometimes together with leukocytosis, with a long latency (Figures 5a, c and d, and Table 1). In addition, to examine the possibility that the phenotypes associated with STAT5A#2 might change, similar to oncogenic *NRAS*, the BM cells transduced with STAT5A#2 (in pMYs-IRES-EGFP) and/or *MLL-SEPT6* (in pMXs-neo) were again transplanted into recipient mice under sublethal conditioning. Within an observation period of 160 days, two of three neo/#2 mice under sublethal conditioning died with longer latencies (134 and 139 days) and showed the same phenotype of myeloid hyperplasia in the BM, where a small population (15%) expressed STAT5A#2, although these had different phenotypes of pancytopenia and splenomegaly (Supplementary Figure 3b and data not shown). In contrast, two of three MS6/#2 mice and all of the three MS6/GFP mice survived and showed no hematological abnormalities in the peripheral blood, whereas one of the MS6/#2 mice died (125 day) but could not be analyzed because of post-mortem change, within the observation period. Histopathological analysis of one MS6/#2 mouse, which was killed 150 days after the transplantation, showed no significant hepatosplenomegaly but mild myeloid hyperplasia in the BM (data not shown). Only 30% of the BM cells were positive for donor-derived Ly-5.1, and 7% of the BM cells were positive for GFP, indicating expression of STAT5A#2 (Supplementary Figure 3c), whereas reverse transcriptase-PCR analysis of the BM cells gave very weak signals of *MLL-SEPT6* after 30 cycles (data not shown), but clearly visible signals after 35 cycles (Supplementary Figure 3c). Therefore, sublethal conditioning seemed to be inappropriate for leukemogenesis assays using oncogenes, such as *MLL-SEPT6* and STAT5A#2, which had relatively weak oncogenic potential in comparison with *MLL-ENL* and $NRAS^{G12V}$.

Finally, we examined whether *Hoxa9* may be involved in cooperation between the *MLL* fusion protein and oncogenic *NRAS in vivo*, such as in transformation assays *in vitro*. The leukemogenesis assays using the BM cells transduced with

Hoxa9 and oncogenic *NRAS* were carried out under lethal conditioning, because preliminary leukemogenesis assays under sublethal conditioning were unsuccessful probably because of engraftment failure (data not shown). The combination of *Hoxa9* and *NRAS*^{G12V} (A9/G12V) led to death with short latencies (28 ± 7.5 days) (Figure 6a and Table 1), whereas *Hoxa9* (and GFP) *per se* induced no lethal disease within 120 days, as reported earlier.[37] The A9/G12V mice showed remarkable hepatosplenomegaly and had a tendency toward leukocytosis, anemia and thrombocytopenia (Table 1). Histopathological and immunophenotyping analyses of the BM cells revealed that the A9/G12V mice had a few, but prominent, myelomonocytic blasts (Figure 6b), with high expression of CD11b and Gr-1, and low level of c-Kit (Figure 6c). A Southern blot analysis of genomic DNAs derived from the spleens of the A9/G12V mice gave oligoclonal bands (data not shown). These results indicated that *Hoxa9* cooperated with oncogenic *NRAS* to rapidly induce lethal myeloid malignancy that was not identical but similar to the acute leukemia induced by *MLL* fusion proteins and oncogenic *NRAS*.

Taken together, these results *in vivo* suggested that *MLL* fusion proteins rapidly induce acute leukemia together with activated *NRAS*, at least in part through aberrant expression of *Hoxa9*.

Discussion

The present study provides several evidences that *MLL*-fusion-mediated leukemogenesis cooperated synergistically with Ras activation, but not with STAT5 activation. Although all known *MLL* fusion proteins were not tested in this study, we showed that this synergistic cooperation was not limited to the specific *MLL* fusion, using two different well-characterized types of *MLL* fusion proteins. In the light of the role of FLT3 mutations in *MLL*-fusion-mediated leukemogenesis described earlier,[6] signaling pathways downstream of FLT3 mutations were analyzed in the transfectants of HF6, a cell line expressing *MLL-SEPT6*. The immortalized cells, such as HF6 and A9G, used in this study might have acquired additional mutations. However, the phenotypes including IL-3 dependency, expression patterns of lineage markers and growth rates were not changed since their establishment (data not shown), thus suggesting that at least no mutations leading to critical transformation had occurred in these cell lines. Although recent studies have disclosed the differences in activation of signal molecules, including MAPK and STAT5, between *FLT3*-TKD and *FLT3*-ITD,[24,38] our experiments using transduction with FLT3 mutants and inhibition of the signal molecules first showed a crucial role of activation of MAPK rather than STAT5 in the factor-independent survival and proliferation of HF6 cells. Next, the myeloid transformation assays *in vitro* revealed that the activation of Raf-1, as well as oncogenic *NRAS*, transformed HF6 cells, but that constitutively active mutants (1*6 and #2) of STAT5A did not. The leukemogenesis assays *in vivo* also showed that oncogenic *NRAS* rapidly induced acute leukemia together with *MLL* fusion proteins, which differed from the original phenotype induced by each molecule. In contrast, the active STAT5A mutant did not confer obvious synergistic effects on the *MLL*-fusion-mediated leukemogenesis. Thus, these results *in vitro* and *in vivo* suggested that activation of the Ras/Raf/MAPK pathway may be sufficient for the transformation of HF6 cells and development of *MLL*-fusion-mediated leukemia.

Oncogenic *NRAS* induced thymoma in the leukemogenesis assays under sublethal conditioning, which is consistent with the

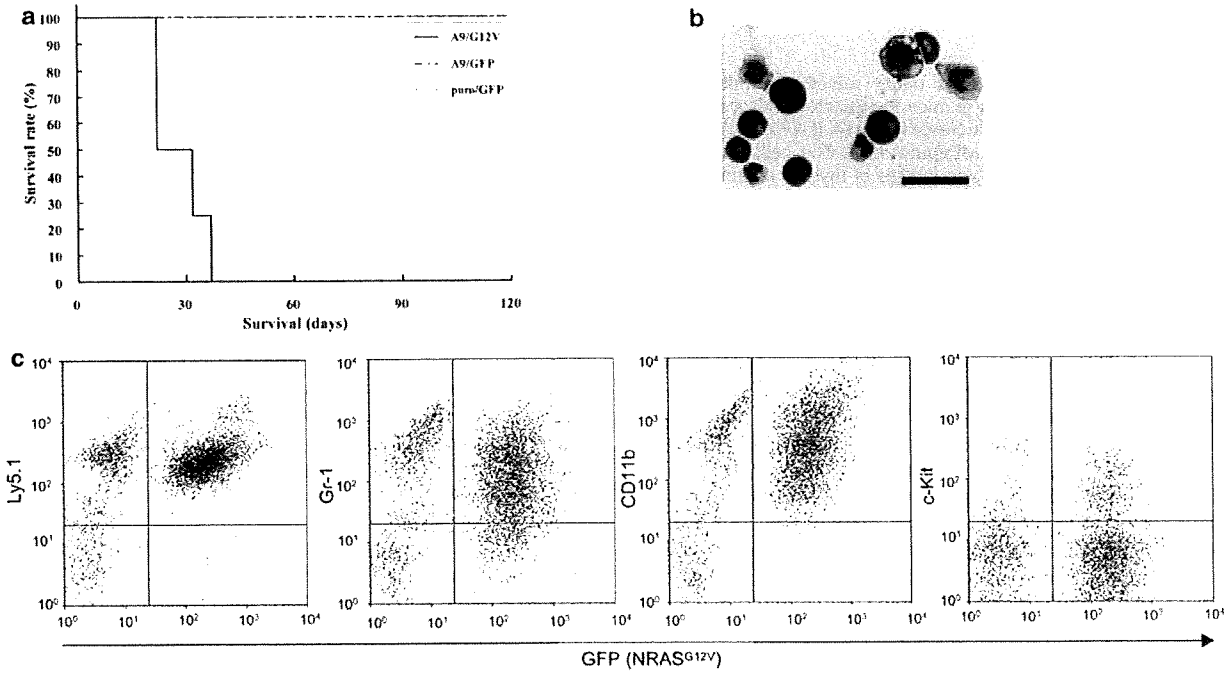

Figure 6 Leukemogenesis induced by *Hoxa9* and oncogenic neuroblastoma RAS viral (v-ras) oncogene homolog (*NRAS*) under lethal conditioning. (**a**) Survival curves of mice transplanted with *Hoxa9* and *NRAS*^{G12V} (A9/G12V; $n = 4$), A9/green fluorescent protein (GFP) ($n = 6$) and puro/GFP ($n = 3$). (**b**) Representative cytospin preparations of bone marrow (BM) cells obtained from morbid A9/G12V mice. The cells were stained with Wright-Giemsa. Original magnification, × 200; scale bar, 30 μm. (**c**) Immunophenotype of BM cells obtained from representative morbid A9/G12V mice. The dot plots show each surface antigen labeled with a corresponding monoclonal antibody versus expression of GFP. Ly5.1, Gr-1, CD11b, and c-Kit were labeled with phycoerythrin (PE)-conjugated and allophycocyanin (APC)-conjugated monoclonal antibodies, respectively.

development of T-lymphoma by *FLT3*-TKD in our experimental system (Ono *et al.*, unpublished data), whereas it led to the development of BM aplasia in our leukemogenesis assays under lethal conditioning. This difference in the disease phenotypes implies that forced expression of oncogenic *NRAS* in BM progenitors might be involved in its inhibitory effects on the engraftment of radioprotective cells as well as the antiproliferative effect of oncogenic *NRAS* in the early phase of the transplantation.[39] These disease phenotypes were also different from the development of MPD in the earlier reports.[39,40] This discrepancy might be due to the differences in the experimental systems, such as the retroviral transduction and mice strains. Meanwhile, the BM progenitors transduced with *Hoxa9* and $NRAS^{G12V}$ seemed to result in engraftment failure under sublethal conditioning, but these rapidly developed myeloid malignancy under lethal conditioning. A recent study using BM transplantation showed the possibility of drastic fluctuation in the engraftment of donor cells receiving pathological modification under sublethal conditioning;[41] hence, our unsuccessful results under sublethal conditioning might be associated with some instability of the transplantation.

Our leukemogenesis assays showed a definitively synergistic cooperation between *MLL* fusion proteins and oncogenic *NRAS* in the acceleration of disease onset and change of the phenotypes. Interestingly, the synergistic cooperation between *MLL* fusion proteins and Ras/Raf/MAPK activation closely correlated with recent clinical studies reporting the frequent coincidence of *MLL* fusion genes and mutations of *RAS*[20] or *RAF*.[42] It was reported that the additional expression of oncogenic *KRAS* induced an acute promyelocytic leukemia-like disease in transgenic mice expressing promyelocytic leukemia/retinoic acid receptor-α with an increased penetrance and decreased latency, although neither the penetrance nor the latency was significantly different from those in mice that died of MPD by expression of oncogenic *KRAS* alone.[43] Other groups recently reported that the combination of oncogenic *NRAS* and *MLL-AF9*[44] or *MLL-ENL*[45] is capable of developing *AML*, and that induced repression of oncogenic *NRAS* on the combination reverted *AML* to MPD by the *MLL* fusion gene (*MLL-AF9*) alone.[44] Although our findings that *MLL* fusion proteins and oncogenic *NRAS* cooperate to induce *AML* confirmed these notions, the present study further analyzed the involvement of *Hoxa9* and Raf, downstream of the cooperation between *MLL* fusion proteins and oncogenic *NRAS*. The myeloid transformation assays *in vitro* showed that the activation of Raf-1, as well as oncogenic *NRAS*, transformed A9G, a cell line expressing *Hoxa9*. The leukemogenesis assays *in vivo* also showed that *Hoxa9* and oncogenic *NRAS* rapidly developed myeloid malignancy. These results *in vitro* and *in vivo* suggested that, as downstream molecules, *Hoxa9* and Raf may have important roles in the synergistic leukemogenesis by *MLL* fusion proteins and oncogenic *NRAS*.

Our findings suggest a possible model of *MLL*-fusion-mediated leukemogenesis that was essentially recapitulated by *Hoxa9* expression and Ras/Raf/MAPK activation (Figure 7). In the context of secondary genetic alterations, such as *FLT3* mutations, this model explains the clinical features of acute leukemia with 11q23 translocations. First, overexpression, as well as TKD mutations, of *FLT3* frequently detected in the *MLL*-rearranged infant acute leukemia may be involved in the leukemogenesis mainly through activation of Ras/Raf/MAPK, because several studies reported that the signaling pathway of wild-type *FLT3* is similar to *FLT3*-TKD rather than *FLT3*-ITD.[24,38] Second, besides *FLT3*, other unknown molecular pathways that lead to the activation of Ras/Raf/MAPK might also be involved in

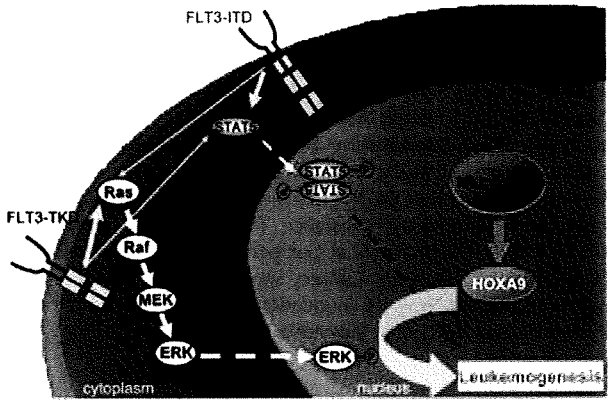

Figure 7 A model of *mixed-lineage-leukemia* (*MLL*)-mediated leukemogenesis together with secondary genetic alterations. *MLL* fusion protein and secondary genetic alterations cooperate to induce acute leukemia through synergistic molecular crosstalk between aberrant expression of *Hox* genes, including *Hoxa9*, and the activation of Ras/Raf/mitogen-activated protein kinase (MAPK). Other signaling pathways, including signal transducer and activator of transcription 5 (STAT5) activation, only additively affect the leukemogenic potential.

the *MLL*-rearranged leukemia carrying no known genetic alterations, as *FLT3* alterations are not found very frequently in most *MLL*-rearranged leukemia except in infants.[46,47] Meanwhile, in the context of *MLL* fusion proteins, we analyzed the role of the *Hoxa9*-mediated pathway leading to leukemogenesis. Recent studies revealed that one of the *Hox*-cofactor molecules, *Meis1*, is an essential molecule involved in normal hematopoiesis[48] as well as *Hoxa9*-mediated leukemogenesis.[49] However, our experimental system[6] using BM cells transduced with *MLL* fusion proteins did not detect any significant upregulation of *Meis1* in comparison with the mock transduction as reported earlier,[50] in contrast with the findings by other groups.[14] Therefore, we focused on *Hoxa9*, one of the key molecules directly upregulated by *MLL* fusion proteins. Interestingly, a recent study showed that the combination of *Hoxa9* and *Meis1* cooperated with *Trib1*, which enhanced the phosphorylation of ERK, to induce acute leukemia in the BM transplantation assays.[51] Their study is not inconsistent with our findings; thus, the *HOX* and Ras/Raf/MAPK axes may have central roles in the molecular network of *MLL*-mediated leukemogenesis, which might be additively affected by other pathways, such as activation of STAT5 (Figure 7). In addition, at least, endogenous expression of *Meis1* in A9G cells is also considered to be important in this network, but further analysis will be required to clarify the role of *Meis1* in the collaboration between *HOX* and MAPK axes.

Conclusion

This study suggests that *MLL* fusion proteins synergistically cooperate with Ras/Raf/MAPK activation in leukemogenesis, at least partly through the upregulation of *Hoxa9*. Future studies analyzing the molecular crosstalk between *Hoxa9* and the Ras/Raf/MAPK cascade are expected to provide novel insights into the molecular mechanism of *MLL*-fusion-mediated leukemogenesis.

Conflict of interest

The authors declare no conflict of interest.

Acknowledgements

We thank Dr Guy Sauvageau (Laboratory of Molecular Genetics of Stem Cells, Institute for Research in Immunology and Cancer, Canada) for the plasmid harboring a fragment of *Hoxa9*, and Dr Yusuke Satoh (Hematology and Oncology, Osaka University Graduate School of Medicine, Osaka, Japan) for technical advice. We are also grateful to R&D Systems for providing cytokines, and Brian Quinn for language assistance. This work was supported in part by Chugai Pharmaceutical Company Ltd, Grants-in-Aid from the Ministry of Education, Culture, Sports, Science, and Technology in Japan, the Novartis Foundation (Japan) for the Promotion of Science and the Japan Leukaemia Research Fund.

References

1 Vogelstein B, Kinzler KW. Cancer genes and the pathways they control. *Nat Med* 2004; **10**: 789–799.
2 Look AT. Oncogenic transcription factors in the human acute leukemias. *Science* 1997; **278**: 1059–1064.
3 Rowley JD. The critical role of chromosome translocations in human leukemias. *Annu Rev Genet* 1998; **32**: 495–519.
4 Gilliland DG, Tallman MS. Focus on acute leukemias. *Cancer Cell* 2002; **1**: 417–420.
5 Kelly LM, Kutok JL, Williams IR, Boulton CL, Amaral SM, Curley DP *et al.* PML/RARalpha and FLT3-ITD induce an APL-like disease in a mouse model. *Proc Natl Acad Sci USA* 2002; **99**: 8283–8288.
6 Ono R, Nakajima H, Ozaki K, Kumagai H, Kawashima T, Taki T *et al.* Dimerization of MLL fusion proteins and FLT3 activation synergize to induce multiple-lineage leukemogenesis. *J Clin Invest* 2005; **115**: 919–929.
7 Schessl C, Rawat VP, Cusan M, Deshpande A, Kohl TM, Rosten PM *et al.* The *AML1-ETO* fusion gene and the FLT3 length mutation collaborate in inducing acute leukemia in mice. *J Clin Invest* 2005; **115**: 2159–2168.
8 Stubbs MC, Kim YM, Krivtsov AV, Wright RD, Feng Z, Agarwal J *et al.* MLL-AF9 and FLT3 cooperation in acute myelogenous leukemia: development of a model for rapid therapeutic assessment. *Leukemia* 2008; **22**: 66–77.
9 Watanabe-Okochi N, Kitaura J, Ono R, Harada H, Harada Y, Komeno Y *et al.* AML1 mutations induced MDS and MDS/AML in a mouse BMT model. *Blood* 2008; **111**: 4297–4308.
10 Ayton PM, Cleary ML. Molecular mechanisms of leukemogenesis mediated by MLL fusion proteins. *Oncogene* 2001; **20**: 5695–5707.
11 Meyer C, Kowarz E, Hofmann J, Renneville A, Zuna J, Trka J *et al.* New insights to the MLL recombinome of acute leukemias. *Leukemia* 2009; **23**: 1490–1499.
12 Yokoyama A, Somervaille TC, Smith KS, Rozenblatt-Rosen O, Meyerson M, Cleary ML. The menin tumor suppressor protein is an essential oncogenic cofactor for MLL-associated leukemogenesis. *Cell* 2005; **123**: 207–218.
13 Daser A, Rabbitts TH. Extending the repertoire of the *mixed-lineage leukemia* gene *MLL* in leukemogenesis. *Genes Dev* 2004; **18**: 965–974.
14 Hess JL. MLL: a histone methyltransferase disrupted in leukemia. *Trends Mol Med* 2004; **10**: 500–507.
15 Corral J, Lavenir I, Impey H, Warren AJ, Forster A, Larson TA *et al.* An *MLL-AF9* fusion gene made by homologous recombination causes acute leukemia in chimeric mice: a method to create fusion oncogenes. *Cell* 1996; **85**: 853–861.
16 Drynan LF, Pannell R, Forster A, Chan NM, Cano F, Daser A *et al.* MLL fusions generated by Cre-loxP-mediated *de novo* translocations can induce lineage reassignment in tumorigenesis. *EMBO J* 2005; **24**: 3136–3146.
17 Wang J, Iwasaki H, Krivtsov A, Febbo PG, Thorner AR, Ernst P *et al.* Conditional *MLL-CBP* targets GMP and models therapy-related myeloproliferative disease. *EMBO J* 2005; **24**: 368–381.
18 Chen W, Li Q, Hudson WA, Kumar A, Kirchhof N, Kersey JH. A murine *MLL-AF4* knock-in model results in lymphoid and myeloid deregulation and hematologic malignancy. *Blood* 2006; **108**: 669–677.
19 Taketani T, Taki T, Sugita K, Furuichi Y, Ishii E, Hanada R *et al.* FLT3 mutations in the activation loop of tyrosine kinase domain are frequently found in infant ALL with *MLL* rearrangements and pediatric ALL with hyperdiploidy. *Blood* 2004; **103**: 1085–1088.
20 Liang DC, Shih LY, Fu JF, Li HY, Wang HI, Hung IJ *et al.* K-Ras mutations and N-Ras mutations in childhood acute leukemias with or without mixed-lineage leukemia gene rearrangements. *Cancer* 2006; **106**: 950–956.
21 Gilliland DG, Griffin JD. The roles of FLT3 in hematopoiesis and leukemia. *Blood* 2002; **100**: 1532–1542.
22 Armstrong SA, Staunton JE, Silverman LB, Pieters R, den Boer ML, Minden MD *et al.* *MLL* translocations specify a distinct gene expression profile that distinguishes a unique leukemia. *Nat Genet* 2002; **30**: 41–47.
23 Murata K, Kumagai H, Kawashima T, Tamitsu K, Irie M, Nakajima H *et al.* Selective cytotoxic mechanism of GTP-14564, a novel tyrosine kinase inhibitor in leukemia cells expressing a constitutively active Fms-like tyrosine kinase 3 (FLT3). *J Biol Chem* 2003; **278**: 32892–32898.
24 Choudhary C, Schwable J, Brandts C, Tickenbrock L, Sargin B, Kindler T *et al.* AML-associated Flt3 kinase domain mutations show signal transduction differences compared with Flt3 ITD mutations. *Blood* 2005; **106**: 265–273.
25 Nosaka T, Kawashima T, Misawa K, Ikuta K, Mui AL, Kitamura T. STAT5 as a molecular regulator of proliferation, differentiation and apoptosis in hematopoietic cells. *EMBO J* 1999; **18**: 4754–4765.
26 Schubbert S, Shannon K, Bollag G. Hyperactive Ras in developmental disorders and cancer. *Nat Rev Cancer* 2007; **7**: 295–308.
27 Ariyoshi K, Nosaka T, Yamada K, Onishi M, Oka Y, Miyajima A *et al.* Constitutive activation of STAT5 by a point mutation in the SH2 domain. *J Biol Chem* 2000; **275**: 24407–24413.
28 Onishi M, Nosaka T, Misawa K, Mui AL, Gorman D, McMahon M *et al.* Identification and characterization of a constitutively active STAT5 mutant that promotes cell proliferation. *Mol Cell Biol* 1998; **18**: 3871–3879.
29 Kitamura T, Koshino Y, Shibata F, Oki T, Nakajima H, Nosaka T *et al.* Retrovirus-mediated gene transfer and expression cloning: powerful tools in functional genomics. *Exp Hematol* 2003; **31**: 1007–1014.
30 Kroon E, Krosl J, Thorsteinsdottir U, Baban S, Buchberg AM, Sauvageau G. Hoxa9 transforms primary bone marrow cells through specific collaboration with Meis1a but not Pbx1b. *EMBO J* 1998; **17**: 3714–3725.
31 Sakaue-Sawano A, Kurokawa H, Morimura T, Hanyu A, Hama H, Osawa H *et al.* Visualizing spatiotemporal dynamics of multicellular cell-cycle progression. *Cell* 2008; **132**: 487–498.
32 Calvo KR, Sykes DB, Pasillas M, Kamps MP. Hoxa9 immortalizes a granulocyte-macrophage colony-stimulating factor-dependent promyelocyte capable of biphenotypic differentiation to neutrophils or macrophages, independent of enforced meis expression. *Mol Cell Biol* 2000; **20**: 3274–3285.
33 Ono R, Ihara M, Nakajima H, Ozaki K, Kataoka-Fujiwara Y, Taki T *et al.* Disruption of *Sept6*, a fusion partner gene of *MLL*, does not affect ontogeny, leukemogenesis induced by *MLL-SEPT6*, or phenotype induced by the loss of *Sept4*. *Mol Cell Biol* 2005; **25**: 10965–10978.
34 Nosaka T, van Deursen JM, Tripp RA, Thierfelder WE, Witthuhn BA, McMickle AP *et al.* Defective lymphoid development in mice lacking Jak3. *Science* 1995; **270**: 800–802.
35 Moriggl R, Gouilleux-Gruart V, Jähne R, Berchtold S, Gartmann C, Liu X *et al.* Deletion of the carboxyl-terminal transactivation domain of MGF-STAT5 results in sustained DNA binding and a dominant negative phenotype. *Mol Cell Biol* 1996; **16**: 5691–5700.
36 Schwaller J, Parganas E, Wang D, Cain D, Aster JC, Williams IR *et al.* STAT5 is essential for the myelo- and lymphoproliferative disease induced by TEL/JAK2. *Mol Cell* 2000; **6**: 693–704.
37 Nakamura T, Largaespada DA, Shaughnessy Jr JD, Jenkins NA, Copeland NG. Cooperative activation of Hoxa and Pbx1-related genes in murine myeloid leukaemias. *Nat Genet* 1996; **12**: 149–153.
38 Grundler R, Miething C, Thiede C, Peschel C, Duyster J. FLT3-ITD and tyrosine kinase domain mutants induce 2 distinct phenotypes in a murine bone marrow transplantation model. *Blood* 2005; **105**: 4792–4799.

39 MacKenzie KL, Dolnikov A, Millington M, Shounan Y, Symonds G. Mutant N-ras induces myeloproliferative disorders and apoptosis in bone marrow repopulated mice. *Blood* 1999; **93**: 2043–2056.
40 Parikh C, Subrahmanyam R, Ren R. Oncogenic NRAS rapidly and efficiently induces CMML- and AML-like diseases in mice. *Blood* 2006; **108**: 2349–2357.
41 Santaguida M, Schepers K, King B, Sabnis AJ, Forsberg EC, Attema JL *et al.* JunB protects against myeloid malignancies by limiting hematopoietic stem cell proliferation and differentiation without affecting self-renewal. *Cancer Cell* 2009; **15**: 341–352.
42 Christiansen DH, Andersen MK, Desta F, Pedersen-Bjergaard J. Mutations of genes in the receptor tyrosine kinase (RTK)/RAS-BRAF signal transduction pathway in therapy-related myelodysplasia and acute myeloid leukemia. *Leukemia* 2005; **19**: 2232–2240.
43 Chan IT, Kutok JL, Williams IR, Cohen S, Moore S, Shigematsu H *et al.* Oncogenic K-ras cooperates with PML-RAR alpha to induce an acute promyelocytic leukemia-like disease. *Blood* 2006; **108**: 1708–1715.
44 Kim WI, Matise I, Diers MD, Largaespada DA. RAS oncogene suppression induces apoptosis followed by more differentiated and less myelosuppressive disease upon relapse of acute myeloid leukemia. *Blood* 2009; **113**: 1086–1096.
45 Zuber J, Radtke I, Pardee TS, Zhao Z, Rappaport AR, Luo W *et al.* Mouse models of human AML accurately predict chemotherapy response. *Genes Dev* 2009; **23**: 877–889.
46 Chillon MC, Fernandez C, Garcia-Sanz R, Balanzategui A, Ramos F, Fernandez-Calvo J *et al.* FLT3-activating mutations are associated with poor prognostic features in AML at diagnosis but they are not an independent prognostic factor. *Hematol J* 2004; **5**: 239–246.
47 Bacher U, Haferlach C, Kern W, Haferlach T, Schnittger S. Prognostic relevance of FLT3-TKD mutations in AML: the combination matters–an analysis of 3082 patients. *Blood* 2008; **111**: 2527–2537.
48 Hisa T, Spence SE, Rachel RA, Fujita M, Nakamura T, Ward JM *et al.* Hematopoietic, angiogenic and eye defects in Meis1 mutant animals. *EMBO J* 2004; **23**: 450–459.
49 Wong P, Iwasaki M, Somervaille TC, So CW, Cleary ML. Meis1 is an essential and rate-limiting regulator of MLL leukemia stem cell potential. *Genes Dev* 2007; **21**: 2762–2774.
50 Horton SJ, Grier DG, McGonigle GJ, Thompson A, Morrow M, De Silva I *et al.* Continuous MLL-ENL expression is necessary to establish a 'Hox Code' and maintain immortalization of hematopoietic progenitor cells. *Cancer Res* 2005; **65**: 9245–9252.
51 Jin G, Yamazaki Y, Takuwa M, Takahara T, Kaneko K, Kuwata T *et al.* Trib1 and Evi1 cooperate with Hoxa and Meis1 in myeloid leukemogenesis. *Blood* 2007; **109**: 3998–4005.

Supplementary Information accompanies the paper on the Leukemia website (http://www.nature.com/leu)

Int J Hematol (2009) 89:470–481
DOI 10.1007/s12185-009-0299-0

ORIGINAL ARTICLE

Possible involvement of RasGRP4 in leukemogenesis

Naoko Watanabe-Okochi · Toshihiko Oki · Yukiko Komeno · Naoko Kato · Koichiro Yuji · Ryoichi Ono · Yuka Harada · Hironori Harada · Yasuhide Hayashi · Hideaki Nakajima · Tetsuya Nosaka · Jiro Kitaura · Toshio Kitamura

Received: 25 January 2009 / Revised: 24 February 2009 / Accepted: 8 March 2009 / Published online: 7 April 2009

Abstract It is now conceivable that leukemogenesis requires two types of mutations, class I and class II mutations. We previously established a mouse bone marrow-derived HF6, an IL-3-dependent cell line, that was immortalized by a class II mutation MLL/SEPT6 and can be fully transformed by class I mutations such as FLT3 mutants. To understand the molecular mechanism of leukemogenesis, particularly progression of myelodysplastic syndrome (MDS) to acute leukemia, we made cDNA libraries from the samples of patients and screened them by expression-cloning to detect class I mutations that render HF6 cells factor-independent. We identified RasGRP4, an activator of Ras, as a candidate for class I mutation from three of six patients (MDS/MPD = 1, MDS-RA = 1, MDS/AML = 2, CMMoL/AML = 1 and AML-M2 = 1). To investigate the potential roles of RasGRP4 in leukemogenesis, we tested its in vivo effect in a mouse bone marrow transplantation (BMT) model. C57BL/6J mice transplanted with RasGRP4-transduced primary bone marrow cells died of T cell leukemia, myeloid leukemia, or myeloid leukemia with T cell leukemia. To further examine if the combination of class I and class II mutations accelerated leukemic transformation, we performed a mouse BMT model in which both AML1 mutant (S291fsX300) and RasGRP4 were transduced into bone marrow cells. The double transduction led to early onset of T cell leukemia but not of AML in the transplanted mice when compared to transduction of RasGRP4 alone. Thus, we have identified RasGRP4 as a gene potentially involved in leukemogenesis and suggest that RasGRP4 cooperates with AML1 mutations in T cell leukemogenesis as a class I mutation.

Keywords RasGRP4 · AML1 · Class I mutation · Leukemogenesis · cDNA library

Electronic supplementary material The online version of this article (doi:10.1007/s12185-009-0299-0) contains supplementary material, which is available to authorized users.

N. Watanabe-Okochi · T. Oki · Y. Komeno · N. Kato · H. Nakajima · J. Kitaura · T. Kitamura (✉)
Division of Cellular Therapy, Advanced Clinical Research Center, The Institute of Medical Science, The University of Tokyo, 4-6-1 Shirokanedai, Minato-ku, Tokyo 108-8639, Japan
e-mail: kitamura@ims.u-tokyo.ac.jp

K. Yuji
Division of Molecular Therapy, Advanced Clinical Research Center, The Institute of Medical Science, The University of Tokyo, Tokyo, Japan

R. Ono · T. Nosaka
Department of Microbiology, Mie University Graduate School of Medicine, Tsu-shi, Japan

Y. Harada
International Radiation Information Center, Research Institute for Radiation Biology and Medicine, Hiroshima University, Hiroshima, Japan

H. Harada
Department of Hematology and Oncology, Research Institute for Radiation Biology and Medicine, Hiroshima University, Hiroshima, Japan

Y. Hayashi
Department of Hematology/Oncology, Gunma Children's Medical Center, Shibukawa, Japan

1 Introduction

Various chromosome translocations and gene mutations were known to participate in leukemogenesis. Recently, it was recognized that multiple gene alterations are required

for leukemogenesis; coexistence of chromosomal translocations and gene mutations are frequently found in the same patient. There are some frequent combinations including c-Kit mutations and AML1/ETO [1–6], c-Kit mutations and inv(16) [1, 5–7], Ras mutations and AML1 point mutations [8, 9], FLT3-ITD and AML1 point mutations [10, 11], FLT3 mutations and PML-RARα [12–16], MLL rearrangement and FLT3-TKD [17], MLL rearrangement and Ras mutations [18], and FLT3-ITD and NPM1 mutations [19]. Interestingly, on the other hand, RAS and FLT3 mutations, which are detected in about 50% of patients with de novo AML, are negatively associated with each other [20, 21]. In mice models, while expression of PML/RARα in transgenic mice caused a nonfatal myeloproliferative syndrome, transplantation of bone marrow cells obtained from PML/RARα transgenic mice retrovirally transduced with FLT3-ITD resulted in development of an APL-like disease in a short latency [22]. Two step leukemogenesis was also suggested by an in vitro culture system of human hematopoietic cells [23]. Based on these findings, leukemia-related mutations are classified into two groups, class I and class II mutations. Class I mutations include activating mutations of tyrosine kinases and a small GTPase Ras or inactivation of apoptosis-related molecule, and these mutations induce cell proliferation or block apoptosis. On the other hand, class II mutations include dominant negative mutations of transcription factors involved in differentiation of hematopoietic cells, such as AML1/ETO, PML/RARa, or constitutively activated mutations of chromosome remodeling factors such as MLL-related fusion genes [24]. Indeed, it has been reported that a combination of class I and II mutations such as PML/RARα plus FLT3-ITD [22], AML1/ETO plus FLT3 mutation [25], AML1/EVI1 plus BCR/ABL [26], MLL/SEPT6 plus FLT3 mutation [27], K-ras plus PML/RARα [28] induced AML in a mouse BMT model, while either class I or II mutation alone led to, myeloproliferative disorders (MPD) or MDS like disease, not leukemia [22–28].

To identify class I mutations from patients with MDS/AML, MPD, or AML, we used retrovirus-mediated expression cloning; cDNA libraries from patients' samples were constructed and retrovirally transfected into an IL-3-dependent myeloid cell line, HF6, immortalized by a class II mutation MLL/SEPT6 [27]. We searched for class I mutations that abrogate IL-3 dependency of HF6 and we identified RasGRP4 as a candidate gene from three different libraries (MDS/MPD = 1, MDS/AML = 1, MDS-RA = 1). In addition, FLT3-ITD was identified in a patient with MDS/AML.

RasGRP4 belongs to a family of guanine nucleotide-exchange factors (RasGRP1-4) that positively regulate Ras and related small GTPases, and is mainly expressed in myeloid cells and mast cells [29, 30]. RasGRP4 appears to act downstream of the tyrosine kinase receptor c-Kit/CD117 [30]. RasGRP4 is located on 19q13.1 and alterations of this site have been found in several cancers (the "Cancer Chromosomes" at the NCI web site), and was previously isolated by expression cloning from cytogenetically normal AML patients using the focus-forming assay of NIH3T3 cells [29]. In the present study, we isolated RasGRP4 using expression cloning as a gene that fully transforms IL-3-dependent HF6 cells, and investigated the effect of RasGRP4 overexpression in a mouse BMT model and implicated RasGRP4 in leukemogenesis.

2 Materials and methods

2.1 Cell lines and cell culture

A mouse pro-B line Ba/F3 was maintained in RPMI1640/10% fetal bovine serum (FBS) containing 1 ng/ml recombinant mouse IL-3 (obtained from R & D systems). HF6, which had been established by introducing MLL/SEPT6 into mouse bone marrow cells, was maintained in RPMI1640/10% FBS containing 10 ng/ml mouse IL-3 as described [27].

2.2 Screening of cDNA libraries

Complementary cDNA libraries were generated from patients leukemic or MDS cells (MDS/MPD = 1, MDS/AML = 2, CMMoL/AML = 1, MDS-RA = 1, AML-M2 = 1) as described [31]. MDS or leukemic cells of these patients did not harbor recurrent chromosomal translocations involving AML1 or MLL. One patient with AML-M2 did not display t(8;21). The point mutations of AML1 were not screened. Recombinant retroviruses were generated by transient transfection using an ecotropic packaging cell line PLAT-E as described with minor modifications [32]. Bone marrow or peripheral blood samples of patients were taken under the experimental procedure approved by the ethical committees of our institute (approve no. 20-9).

We introduced each cDNA library into two IL-3-dependent cell lines Ba/F3 and HF6. After transduction with the cDNA library, the transduced cells were seeded into 96-well plates in the absence of IL-3, and factor independent clones were isolated. To identify the cDNA that confers factor independency on Ba/F3 or HF6, genomic DNA of the factor independent clones were purified and integrated cDNAs were isolated and sequenced.

2.3 Vector construction

cDNAs for human RasGRP4 were cloned from cDNA libraries of MDS/MPD patients and normal volunteers using PCR primers: 5′-GGAGCTGAGCCCTACTCTTG-3′

(forward), 5′-AGAGTCTGACGGCAGGACTC-3′ (reverse). We used pfu polymerase (Stratagene, La Jolla, CA) to amplify the coding region of human RasGRP4. We subcloned the PCR products into TOPO vector (Invitrogen, San Diego, CA). Then, the EcoRI fragment carrying RasGRP4 was inserted into the EcoRI sites of pMXs vector [32]. RasGRP4 sequences derived from patients and normal volunteers were not identical to those in the data bases as described in result section. We used an AML1 mutant, S291fsX300, identified from case number 27 among MDS/AML patients [33]. This mutant is hereafter referred to as AML1-S291fs. The AML1-S291fs was inserted upstream of the IRES-EGFP cassette of a retrovirus vector pMYs-IG [32] to generate pMYs-AML1-S291fs-IG.

2.4 Expression of RasGRP4 in HF6

To confirm that the isolated RasGRP4 is responsible for factor-independency of HF6, the cells were infected with the retroviruses harboring pMXs-RasGRP4 derived from patients, normal volunteers or an empty vector as a control, and cultured in the absence of IL-3. To investigate the activation of the Ras pathway in the HF6 cells expressing RasGRP4, the transfected cells were lysed in lysis buffer, and lysates were subject to western blot analysis as described with minor modifications [34]. Monoclonal mouse anti-phospho-p44/42 MAPK (Thr^{202}/Tyr^{204}) antibody (Sigma) was used for phosphorylated ERK1/2.

2.5 Bone marrow transplantation

Bone marrow mononuclear cells were isolated and cultured as described [35]. The prestimulated cells were infected for 60 h with the retroviruses harboring pMXs-RasGRP4 derived from a patient with MDS/MPD, pMYs-AML1-S291fs-IG or an empty vector as a control, using six well dishes coated with RetroNectin (Takara Bio, Inc.) according to the manufacturer's recommendations. Then, 0.3–1.2 $\times$ 10^6 of infected bone marrow cells (Ly-5.1) were injected through tail vein into C57BL/6 (Ly-5.2) recipient mice (8–12 weeks of age) which had been administered a sublethal dose of 5.25 Gy total-body γ-irradiation (135Cs). Overall survival of the transplanted mice was analyzed using the Kaplan–Meier-method. All animal studies were approved by the Animal Care Committee of the Institute of Medical Science, The University of Tokyo.

2.6 Analysis of the transplanted mice

Engraftment of bone marrow cells was confirmed by measuring the percentage of Ly-5.1-positive and/or GFP positive cells in peripheral blood obtained every 1–2 months after the transplant. After the morbid mice were euthanized, their tissue samples including peripheral blood (PB), bone marrow (BM), spleen, liver, and kidney were analyzed. Circulating blood cells were counted by automatic blood cell counter KX-21 (Sysmex, Kobe, Japan). Morphology of the peripheral blood cells was evaluated by staining of air-dried smears with Hemacolor (Merck). Tissues were fixed in 10% buffered formalin, embedded in paraffin, sectioned, and stained with hematoxylin and eosin (H & E). Cytospin preparations of bone marrow and spleen cells were also stained with Hemacolor. The percentage of blasts, myelocytes, neutrophils, monocytes, lymphocytes, and erythroblasts was estimated by examination of at least 200 cells. To assess whether the leukemic cells were transplantable, 2 $\times$ 10^5–1 $\times$ 10^6 total BM cells including blasts were injected into the tail veins of sublethally irradiated mice. A total of two or three recipient mice were used for each serial transplantation.

2.7 Flow cytometric analysis

Peripheral blood or single-cell suspensions of bone marrow and spleen were stained with the following phycoerythrin (PE)-conjugated monoclonal antibodies: Ly-5.1, Gr-1, CD11b, B220, CD3, CD4, CD8, CD41, c-Kit, Sca-1, CD34, and Ter-119. Then, flow cytometric analysis was performed as described [35].

2.8 RT-PCR

To confirm expression of human RasGRP4, total RNA was extracted from BM cells of transplanted mice using Trizol (Invitrogen, California, USA) and cDNA was prepared with the Superscript II RT kit (Invitrogen, California, USA) and RT-PCR was performed using a 2720 Thermal cycler (Applied Biosystems, Tokyo, Japan). The cDNA was amplified using AmpliTaq Gold (Applied Biosystems by Roche Molecular Systems, Inc., New Jersey. USA). The reaction was subject to one cycle at 95°C for 5 min, 30 cycles of PCR at 95°C for 30 s, 55°C for 30 s, and 72°C for 30 s. All samples were independently analyzed at least three times. The following primer pairs were used: 5′-ACTGGCTGATGCGACACCC-3′ (forward) and 5′-GAGATGGCACTGTGACACAG-3′ (reverse) for human RasGRP4, 5′-ACCACAGTCCATGCCATCAC-3′ (forward) and 5′-TCCACCACCCTGTTGCTGTA -3′ (reverse) for GAPDH.

2.9 Quantitative RT-PCR

To examine expression levels of human RasGRP4 in patients, quantitative RT-PCR was performed. Quantitative RT-PCR was performed using a LightCycler Workflow System (Roche Diagnostics, Mannheim, Germany).

Complementary DNAs derived from bone marrow cells of leukemia or MDS patients as well as normal bone marrow cells were amplified using a SYBR Premix EX Taq (TAKARA). The reaction was subject to one cycle at 95°C for 30 s, 45 cycles of PCR at 95°C for 5 s, 55°C for 10 s, and 72°C for 10 s. All samples were independently analyzed at least three times. The primer pairs for human RasGRP4 and GAPDH were the same as described above. The samples from the patients were obtained under written consents which had been approved by the local ethical committee of each institute or hospital.

2.10 Bubble PCR

Genomic DNA was extracted from BM or spleen cells of transplanted mice and digested with EcoRI, and then the fragments were used for Bubble PCR to identify the integration sites of the retroviruses as described [35]. We confirmed inverse repeat sequence "GGGGGTCTTTCA" as a marker of junction between genomic DNA and retrovirus sequence.

3 Results

3.1 RasGRP4 induces factor-independent growth of HF6

In the screening of cDNA libraries, some wells gave rise to cell growth in the absence of IL-3 from HF6 but not from BaF3 cells. The factor-independent clones were isolated and the cDNAs integrated in the genome DNA were sequenced using PCR. FLT3-ITD was identified in one MDS/AML patient. In addition, RasGRP4 was identified from three different libraries (MDS/MPD = 1, MDS/AML = 1, and MDS-RA = 1). We introduced the isolated RasGRP4 into HF6 to confirm that RasGRP4 was responsible for autonomous growth of HF6 cells (Fig. 1a). In the sequence of RasGRP4 derived from the MDS/MPD, MDS/AML and MDS-RA patients, we found several different amino acids that compared with the sequences in two databases GenBank (accession number AF448437) and GenBank (accession number AY048119) (Table 1). Therefore, we introduced RasGRP4 derived from a patient and two Japanese normal volunteers (normal 1 and 2 in Table 1) into HF6 cells to examine if RasGRP4 from normal volunteers also gives rise to factor-independency. As a result, RasGRP4 from normal volunteers also induced factor-independent growth of HF6, indicating that overexpression of RasGRP4 by itself induced transformation of the cells, independent of some mutations in the amino acid sequence of RasGRP4. While several gene alterations were observed in the samples of patients, we focused on E468K because this change was observed only in a patient with MDS/MPD but not in the sequence derived from the two databases and two normal volunteers (Table 1). However, we did not find any functional importance of the alteration at codon 468 that changes a glutamic acid to a lysine. Moreover, SNPs of this gene are not correlated with lymphoma and leukemia (Y. Nakamura, unpublished results).

To assess the RasGRP4-mediated Ras activation, we examined phosphorylation of ERK1/2 using HF6-cells-transduced RasGRP4. Stimulation with IL-3 induced much stronger phosphorylation of ERK1/2 in the HF6 cells expressing RasGRP4 when compared with parent HF6 cells (Fig. 1b, lanes 6–8). Although we did not observe enhanced phosphorylation of ERK1/2 in the cells overexpressing RasGRP4 without IL-3 (Fig. 1b, lane 5), we assume that non-detectable enhancement of ERK1/2 was

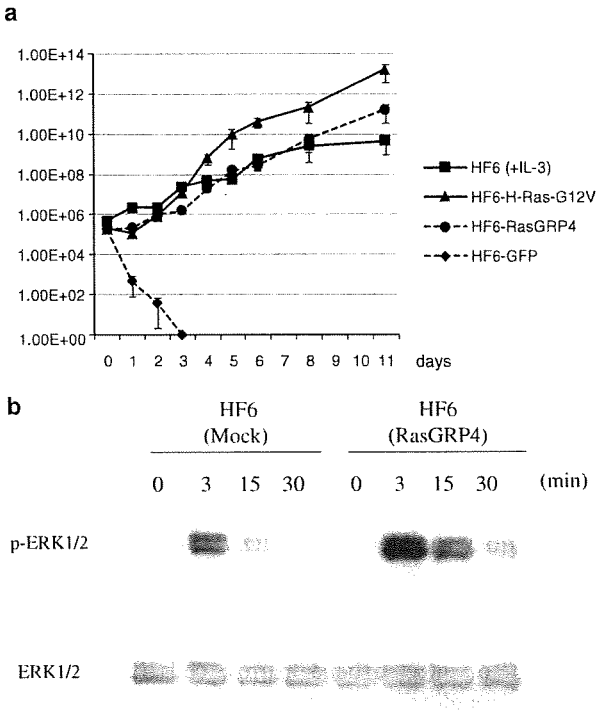

Fig. 1 RasGRP4 conferred factor independency on HF6. **a** HF6 cells expressing the H-Ras-G12V, RasGRP4 and GFP vector were deprived of IL-3, and cells were counted by trypan blue exclusion. The parental HF6 cells in the presence of IL-3 (10 ng/mL) were counted as same. **b** Stimulation with IL-3 induced strong phosphorylation of ERK1/2 in the HF6 cells expressing RasGRP4. Phosphorylation of ERK1/2 (pERK1/2) was examined in HF6 cells transfected with RasGRP4 or empty by western blot analysis using anti-phospho-p44/42 MAPK (Thr^{202}/Tyr^{204}) Ab. Loading amount was estimated by re-probing immunoblots with Abs specific for ERK1/2. The transfected HF6 cells were washed with PBS twice and cultured in RPMI1640/10% FBS without IL-3 for 4 h. Then, some of cells were collected and lysed (*lanes 1 and 5*). The remained cells were stimulated with IL-3 (100 ng/mL) for the indicated period and collected and lysed (*lanes 2–4*, and *6–8*)

Table 1 Polymorphism of RasGRP4

Position of amino acid	AF448437	AY048119	Patient 1 (MDS/MPD)	Patient 2 (MDS/AML)	Patient 3 (MDS-RA)	Normal 1	Normal 2
18	T	T	T	I	T	T	I
120	Q	L	Q	Q	Q	Q	Q
261	R	C	R	R	R	R	R
468	E	E	K	E	E	E	E
541	H	H	H	H	H	H	Y
671	L	P	P	L	L	L	L

enough to induce factor-independent growth of HF6. Only weak activation of the signaling molecule, even non-detectable in biochemical experiments, sometimes induces autonomous cell growth.

3.2 RasGRP4 induced myeloid leukemia and T cell leukemia in mice

We further examined if overexpression of RasGRP4 induced leukemia in a mouse BMT model. We confirmed expression of human RasGRP4 in BM cells of transplanted mice by RT-PCR (Fig. 2a). Transduction of RasGRP4 (E468K) induced myeloid and/or T cell leukemia with various phenotypes, and the transplanted mice died within 2–8 months after the transplantation (Fig. 2b). For example, a mouse (ID 402) died of T cell leukemia with thymoma (weight of thymus was 1,416 mg) and hepatosplenomegaly on day 252 after the transplantation. Leukemic cells showed a CD4- and CD8-double-positive phenotype (Fig. 3). One other mouse developed a similar disease (ID 401). Unfortunately, this mouse died on day 224 before we found out. Therefore, we could only confirm hepatosplenomegaly and a giant thymoma after the death. Two mice (ID 407 and 408) died of AML with hepatosplenomegaly on days 47 and 66 after the transplantation. Severe leukocytosis, anemia and thrombocytopenia were observed in a mouse (ID 408), but severe pancytopenia was observed in the other mouse (ID 407). Leukemic cells of the mouse (ID 408) in bone marrow and thymus uniformly expressed Gr1, CD11b, and B220 on their surfaces (Fig. 3). Four of the transplanted mice (ID 403, 404, 405 and 406) developed both myeloid and T cell leukemia with hepatosplenomegaly, and in some cases, thymoma (ID 404, 405 and 406). In the mouse ID 404, both myeloid and T cell leukemia cells were observed in the bone marrow, while peripheral blood was occupied with myeloid leukemia and thymus was occupied with T cell leukemia (Figs. 3, 4). In summary, two mice died of AML after a short latency (days 47 and 66), two mice died of T cell leukemia after a long latency (days 224 and 252), and four mice died of AML and T cell leukemia (days 76, 83, 129, and 248). The

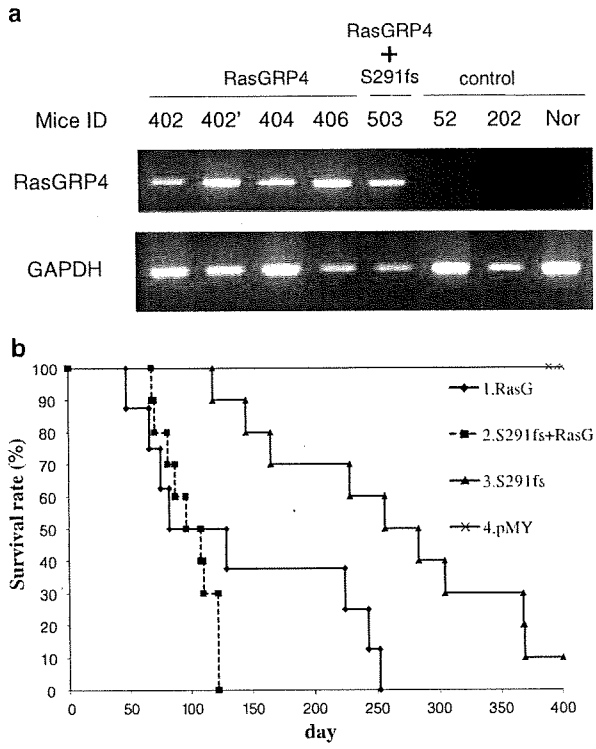

Fig. 2 Co-transduction of RasGRP4 and AML1-S291fs led to early onset of leukemia. **a** Expression of retrovirally introduced RasGRP4 in BM cells. Total RNA from BM cells of transplanted mice were extracted, and the derived cDNAs were subjected to RT-PCR. Mice IDs were shown on the top of the panel. ID 402′ is a second recipient of ID 402. Controls are AML1-S291fs (ID 52), empty vector (ID 202), and normal mouse (Nor). **b** Kaplan–Meier analysis for the survival of mice transplanted with RasGRP4, AML1-S291fs, and double-transduced BM cells. Average survival of RasGRP4 alone (139.8 days) was not significantly different when compared with double transduced mice (101.5 days) ($P = 0.223$, log rank test). Average survival of the double transduced mice (101.5 days) was significantly shorter than that of AML1-S291fs-transduced mice (263.6 days) ($P = 0.00003$, log rank test). RasGRP4 ($n = 8$), AML1-S291fs ($n = 10$), RasGRP4 + AML1-S291fs ($n = 11$), mock ($n = 16$) transduced bone marrow cells were transplanted to mice

details of individual mice are shown in Table 2 and Fig. 5. To assess whether the leukemic cells were transplantable, 2×10^5–1×10^6 total BM cells including blasts were

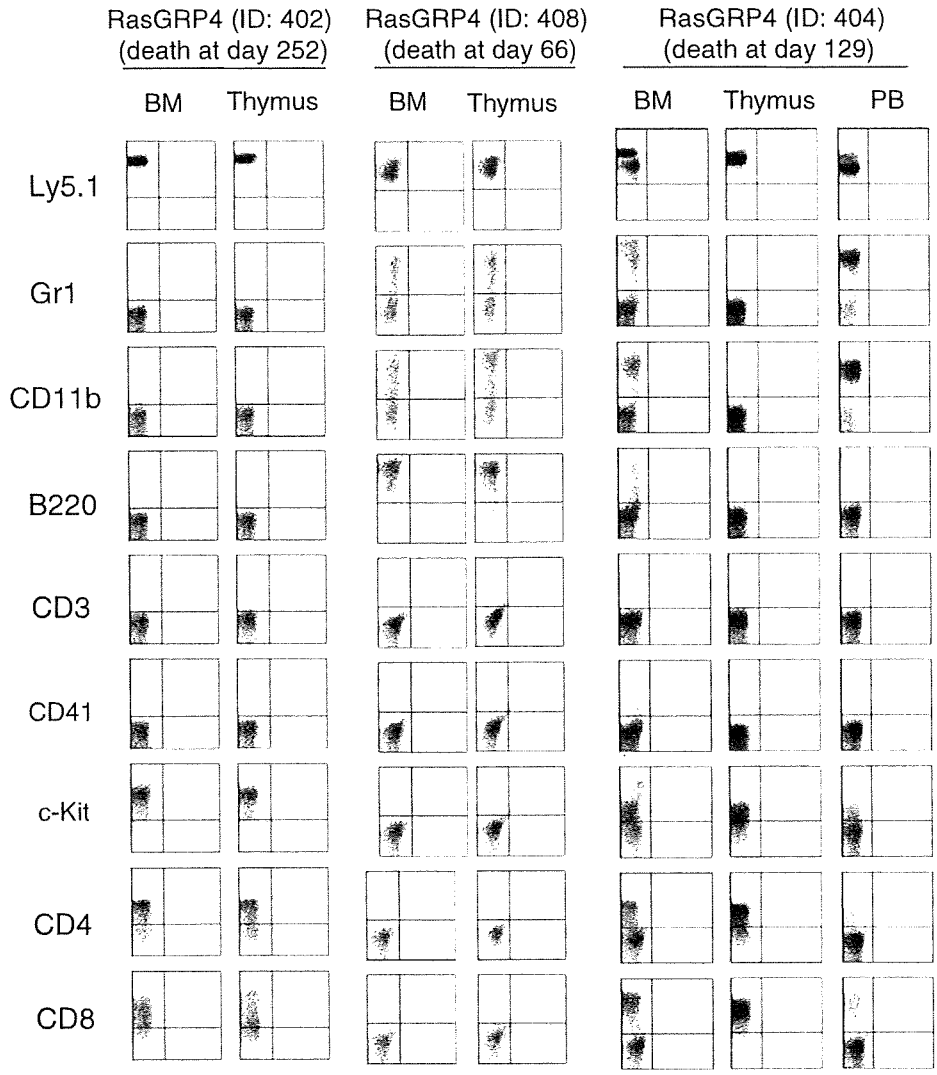

Fig. 3 RasGRP4 induced T cell leukemia and myeloid leukemia in the BMT model. The *dot plots* show Ly5.1, Gr-1, CD11b, B220, CD3, CD41, c-kit, CD4, or CD8 expression detected by corresponding PE-conjugated mAb

injected into recipient mice. We confirmed that both T cell leukemia and myeloid leukemia cells were serially transplantable although the phenotypes slightly changed after the serial transplantation (Supplemental Fig. 1).

3.3 Different integration sites were identified from T cell or myeloid leukemia cells derived from an individual mouse

To examine if the T cell and myeloid leukemia cells were derived from different clones or the same clone, we identified the integration sites in genomic DNA samples of thymus, peripheral blood or bone marrow cells. As shown in Table 3, different integration sites were identified from T cell and myeloid leukemia cells derived from an individual mouse, suggesting that T cell and myeloid leukemic cells were derived from different clones.

The integration near the Samsn1 gene was found twice in ID 405 and ID 406. These mice were transplanted on the same day. The integration site was identical among these leukemic cells indicating that leukemic cells of the two cases were derived from a single hematopoietic progenitor. This result suggests that the integration induced expansion of the transduced stem cells during the 3-day-culture period before the transplantation. Indeed, the mice with the integration at Samsn1 site developed AML with the same phenotype (CD11b positive) and similar latencies (83 and 76 days). On the other hand, different T lineage clones grew up in thymus and developed thymoma.

3.4 RasGRP4 cooperates with an AML1 mutant in leukemogenesis

RasGRP4 appears to function downstream of the tyrosine kinase receptor c-Kit/CD117 [30]. High expression of c-kit

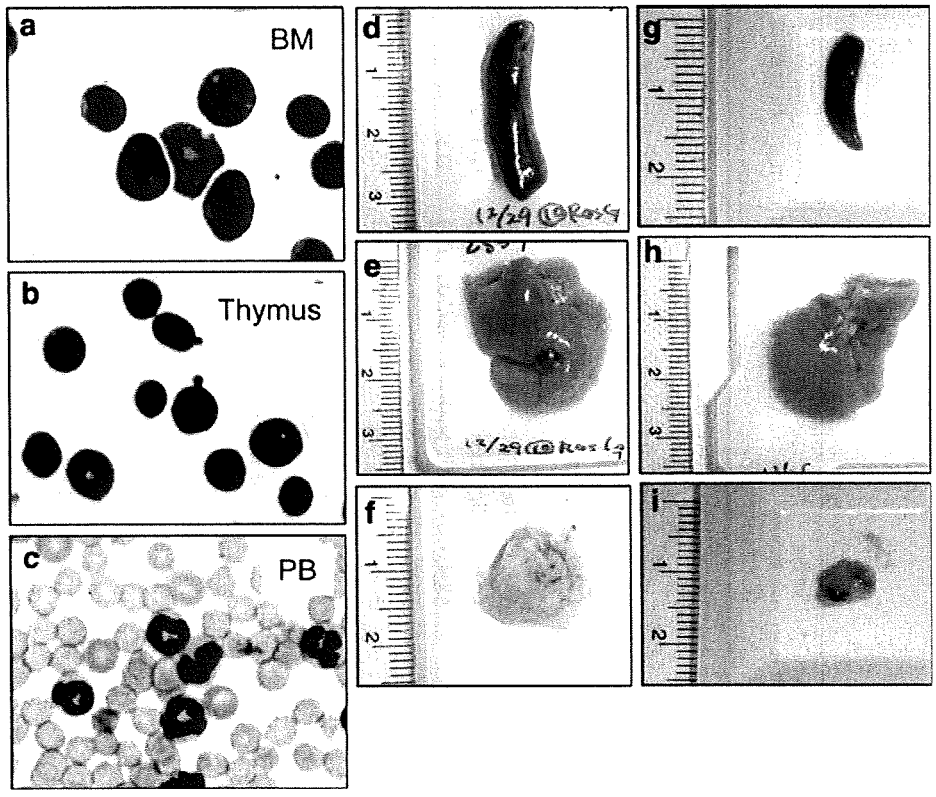

Fig. 4 RasGRP4 induced both of T cell leukemia and myeloid leukemia in the same mouse. Giemsa-stained cells derived from **a** bone marrow, **b** thymus, and **c** peripheral blood obtained from mouse ID 404. Macroscopic findings of **d** spleen, **e** liver, **f** thymus from mice ID 404; *left* **g** spleen, **h** liver, **i** thymus from normal mice; *right* are shown. Images (**a**, **b**, **c**) were obtained with a BH51 microscope and DP12 camera (Olympus, Tokyo, Japan); objective lens, UPlanFl (Olympus); ×1,000

has been found in 60–80% of AML [36] and higher expression is observed in 81.3% of patients with t(8;21) when compared with the patients with other leukemias [2]. Niimi et al. [9] reported that MDS/AML arising from AML1/RUNX1 mutations frequently involves receptor tyrosine kinase (RTK)-RAS signaling pathway activation. We have recently demonstrated that bone marrow cells transduced with AML1 mutants induced MDS-like symptoms after a long latency [35]. Therefore, we also tested if the combination of RasGRP4 and AML1-S291fs, one of the AML1 mutants, induced rapid leukemic transformation in a BMT model. As a result, co-transduction of RasGRP4 and AML1-S291fs led to early death in the transplanted mice (average 101.5 days, $n = 11$) than the expression of RasGRP4 alone (average 139.8 days, $n = 8$) (Fig. 2b). We diagnosed the double-transfected disease mice as T cell leukemia because of enlarged thymus, hepatosplenomegaly, and expansion of blast expressing CD3, CD4, and CD8 in bone marrow, peripheral blood, and thymus (Fig. 6). The onset of T cell leukemia was significantly earlier in the RasGRP4 + AML1 mutant (average 102.7 days, $n = 9$) than RasGRP4 alone (average 238 days, $n = 2$). On the other hand, onset of AML was not significantly changed between RasGRP4 + AML1 mutant (average 96 days, $n = 2$) and RasGRP4 alone (average 56.5 days, $n = 2$) transplanted mice.

3.5 RasGRP4 was overexpressed in some patients with hematological malignancies

We examined expression levels of RasGRP4 in patients with myeloid or T lineage hematological malignancies. As shown in Fig. 7, cells from some patients (T-ALL, AML-M1, MDS-RAEB, MDS-RA, CMMoL) overexpressed RasGRP4.

4 Discussions

We identified RasGRP4 from patients' cDNA libraries as a gene that renders IL-3-dependent HF6 cells factor independent when expressed at high levels via retrovirus-mediated gene transfer. Although we did not find any gain-of-function mutation of RasGRP4 in three patients from whom we identified cDNA for RasGRP4, and we detected high expression of RasGARP4 in only one out of the three patients, it is possible that overexpression or activating mutations are found in patients with malignant diseases including leukemia and MDS. Thus, RasGRP4 is a candidate gene for class I mutations. In addition to RasGRP4, we also identified FLT3-ITD from a patient with MDS/AML, thus showing the feasibility of our functional cloning strategy. The HF6 cells were immortalized by expression

Table 2 Hematological data of the transplanted mice

Gene	Mice ID	GFP (%)	Ly5.1 of BM (%)	Ly5.1 of Thymus (%)	Period from BMT (day)	Spleen weight (mg)	Liver weight (mg)	Thymus weight (mg)	Suefice markers of GFP positive cells	WBC (μL)	Hb (g/dL)	MCV (fL)	Platelet (×1,000/μL)
S291fs	51	27.4	39.8	–	368	153	1,236	–	Gr1, CD11b, CD41, cKit	4,800	6.6	60.0	27.0
S291fs	52	47.8	83.0	–	256	90	1,568	–	Gr1, CD11b, CD41, cKit	4,500	9.9	59.8	38.3
S291fs	54	29.8	45.3	–	304	338	1,812	–	CD11b, CD41, cKit, CD34	1,800	10.4	61.3	4.1
S291fs	55	75.2	83.1	–	165	166	1,574	–	Gr1, CD11b, CD41, cKit,	1,200	4.8	76.4	5.7
S291fs	56	54.9	85.2	–	118	73	1,318	–	CD41, cKit, Sca1, CD34,	2,900	4.5	72.7	4.6
S291fs	57	–	–	–	145	181	1,249	–	–	5,700	2.4		5.1
S291fs	58	72.7	56.5	–	228	225	1,582	–	Gr1, CD11b, CD41, cKit	2,100	9.9	62.7	26.7
S291fs	60	76.3		–	369	186	1,682	–	CD41, c-Kit, CD34	7,500	11.1	66.1	22.2
RasGRP4	402	–	96.5		252	318	1,975		CD4, CD8, c-Kit, Sca1	20,700	12.3	51.9	3.6
				98.9				1,416	CD4, CD8, c-Kit, Sca1				
RasGRP4	403	–	93.5		248	696	2,138		CD41, c-Kit, CD34	8,400	7.2	55.1	0.0
				85.9				92	CD3, CD4, CD8, Sca1				
RasGRP4	404	–	93.9		129	714	2,557		Gr1, CD11b, c-Kit, Sca1, CD4, CD8	282,000	11.7	56.6	3.0
				99.7				777	CD4, CD8, c-Kit, Sca1				
RasGRP4	405	–	91.3		83	1,184	3,699		CD11b	558,900	7.2	57.1	9.9
				98.3				139	CD4, CD8				
RasGRP4	406	–	94.8		76	1,348	2,678		CD11b	96,900	6.6	59.7	1.2
				99.5				609	CD4, CD8				
RasGRP4	407	–	32.0		47	670	4,795		Gr1, CD11b, c-Kit	1,800	4.5	67.6	2.7
				17.1				95	CD3, CD4, CD8				
RasGRP4	408	–	95.7		66	1,110	4,155		Gr1, CD11b, B220	108,900	5.1	104.0	3.9
				93.5				202	Gr1, CD11b, B220				
S291fs + RasGRP4	503	92.1	92.1		96	1,180	6,065		CD3, CD4, CD8	33,600	10.3	64.5	9.3
		95.0		95.0				112	CD3, CD4, CD8				
S291fs + RasGRP4	507	–	–		68	302	–		CD3, CD4, CD8				
				–				805	CD3, CD4, CD8				
S291fs + RasGRP4	513	75.8	80.7		130	544	2,784		CD3, CD8	59,500	10.7	68.8	2.2
		83.8		90.9				155	CD3, CD8				

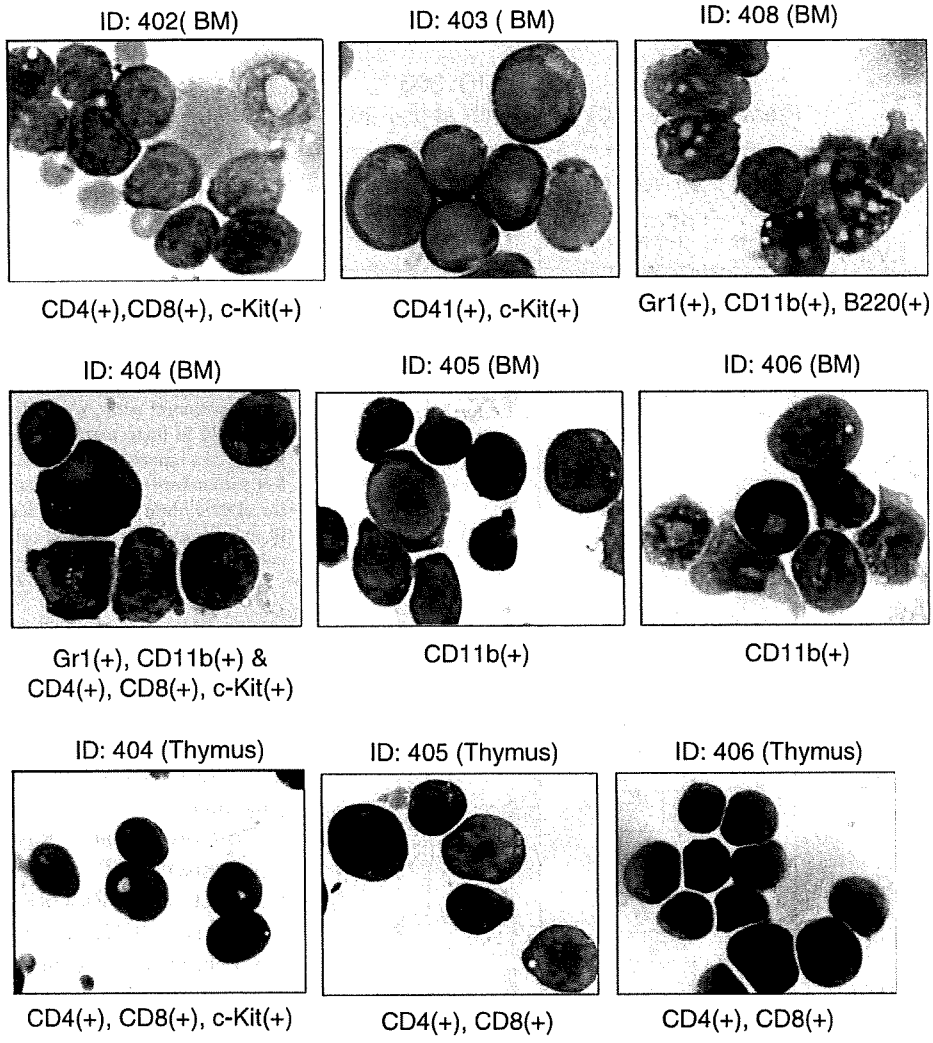

Fig. 5 Morphology of leukemic cells induced by RasGRP4. Giemsa staining photos of the leukemic cells are shown. Mice IDs were shown at *top of the panel*. Surface expression proteins were shown at bottom of the panel. Images were obtained with a BH51 microscope and DP12 camera (Olympus, Tokyo, Japan); objective lens, UPlanFl (Olympus); magnification, ×1,000

Table 3 Retroviral integration sites in the transplanted mice

Mice ID	Sample	Chr. number	Nearest gene	Gene ID	Distance to gene (start or end)	Location	Forward or reverse orientation	RTCGD hits
404	Thymus	10	Bcr	110279	Disrupt CDS	Intron 8	F	0
404	PB	15	Trio	223435	Disrupt CDS	Intron 9	F	3
405	Thymus	14	LOC100042147	100042147	12,962 bp	3′	R	0
405	BM	16	Samsn1	67742	95,998 bp	5′	R	2
406	Thymus	18	LOC100042131	100042131	Disrupt CDS	Exon 2	F	0
406	BM	16	Samsn1	67742	95,998 bp	5′	R	2

of MLL-SEPT6, and can be transformed by oncogenic Ras and Ras-related signals (manuscript in preparation). Therefore, HF6 is a suitable cell line for identification of Ras mutations as well as mutations of Ras-related signaling molecules. On the other hand, Ba/F3 cells can be transformed by STAT5 activation. In addition to these two cell lines, we have developed several other IL-3-dependent bone marrow-derived cell lines immortalized by class II mutations or related molecules (unpublished results). Because these IL-3-dependent cell lines have different signaling profiles, they would be applicable for identification of mutations in a variety of signaling molecules, providing a versatile system for functional cloning of oncogenic mutations.

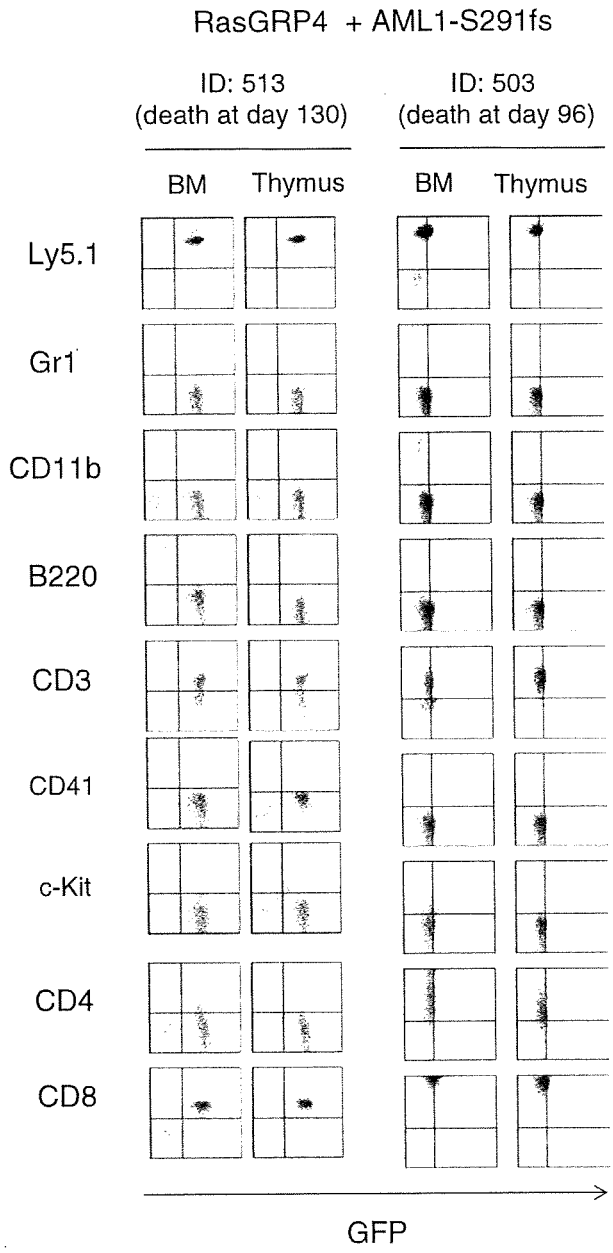

Fig. 6 RasGRP4 and AML1-S291fs induced T cell leukemia in the BMT model. The *dot plots* show Ly5.1, Gr-1, CD11b, B220, CD3, CD41, c-kit, CD4, or CD8 expression detected by corresponding PE-conjugated mAb

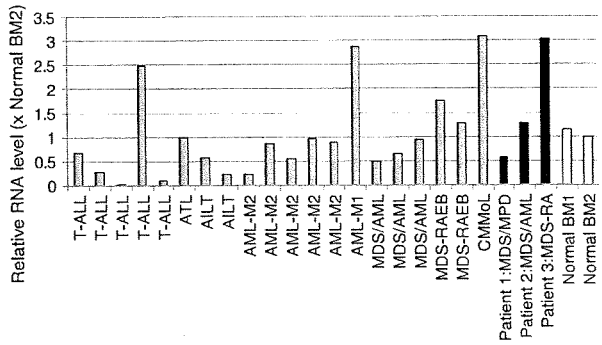

Fig. 7 RasGRP4 was overexpressed in a patient with T-ALL and some patients with myeloid malignancies. Expression levels of RasGRP4 in bone marrow cells derived from patients with hematological malignancies were evaluated by quantitative RT-PCR. *Gray bar* patients with hematological malignancies, *black bar* patients used for cDNA library and identified RasGRP4, *white bar* normal. RNAs from normal bone marrow cells served as a control (RNA level of normal BM2 = 1)

Overexpression of RasGRP4-induced T cell leukemia and/or myeloid leukemia in a mouse BMT model. We found that four of eight mice developed both types of leukemia and two mice died of AML after a short latency, while others died of T cell leukemia after a long latency when transplanted with RasGRP4 alone. At present, it is not clear what determines the different phenotypes of leukemia induced by RasGRP4. Although the retrovirus integration site should modify the outcome, so far we did not find any integration that could explain the differing phenotypes of leukemia. Alternatively, it is also possible that types of progenitors transduced with RasGRP4 determine the different phenotypes of leukemia.

Co-transduction of RasGRP4 and AML1-S291fs led to early onset of T cell leukemia as compared with the transduction of RasGRP4 alone. Putting together with clinical reports [2, 9, 36] and our results, we can suggest the significant association of Ras signaling pathway and function of AML1 mutation in leukemogenesis. While AML1 mutations are frequently associated with myeloid leukemia in human patients, they seemed to shorten the latency of T cell leukemia induced by forced expression of RasGRP4 in mouse BMT model. Intriguingly, while RasGRP4 induced c-Kit+/CD3−/CD4+/CD8+ T cell leukemia, combination of RasGRP4 and AML1-S291fs developed more mature T cell leukemia (c-Kit−/CD3+/CD8+/CD4− or CD4+). The reason for this difference is elusive at present. Although we need more cases of BMT mice for confirmation of this difference, AML1-S291fs may also play some roles to induce T cell differentiation in addition to its overall dominant effects on AML1 transcription. In the clinical cases, AML1-LAF4 [37] and AML1-FGA7 [38] were associated with T-ALL, although most of AML1 translocations are associated with myeloid leukemia. Because AML1 is important for transcription of TCR and silencing of CD4, it is possible that AML1-S291fs inhibited the normal ontogeny of T cells, thus accelerating leukemogenic process caused by RasGRP4 in a mice BMT model as a class II mutation that disturbs T cell ontogeny.